Active Catalysts for Hydrogenation and Dehydrogenation Reactions

M.Sc. Thesis

By

Chanchal Saini

DISCIPLINE OF CHEMISTRY

INDIAN INSTITUTE OF TECHNOLOGY

INDORE

JUNE 2020

Active Catalysts for Hydrogenation and Dehydrogenation Reactions

A THESIS

Submitted in partial fulfilment of the requirements for the award of the degree

of

Master of Science

By

Chanchal Saini

DISCIPLINE OF CHEMISTRY

INDIAN INSTITUTE OF TECHNOLOGY

INDORE

JUNE 2020

INDIAN INSTITUTE OF TECHNOLOGY INDORE

CANDIDATE DECLARATION

I hereby certify that the work which is being presented in the thesis entitled **Active catalysts for hydrogenation and dehydrogenation reactions** in the partial fulfilment of the requirements for the award of the degree of **MASTER OF SCIENCE** and submitted in the **DISCIPLINE OF CHEMISTRY, Indian Institute of Technology Indore**, is an authentic record of my own work carried out during the time period from July 2018 to June 2020 under the supervision of Dr. Sanjay k. Singh, Associate professor, IIT Indore.

The matter presented in this thesis has not been submitted by me for the award of any other degree of this or any other institute.

24/6/20

Chanchal Saini

This is to certify that the above statement made by the candidate is correct to the best of my/our knowledge.

June 24, 2020

Dr. Sanjay K. Singh

Chanchal Saini has successfully given her M.Sc. Oral Examination held on 24.06.2020.

Signature of Supervisor M.Sc. thesis
Date: 24.06.2020

Tushar Kanti Mukherjee

Convener, DPGC
Date: 24.06.2020

Dr. Biswarup Pathak
Signature of PSPC Member
Date: 24.06.2020

M. Shaikh

Signature of PSPC Member
Date: 24.06.2020

Dedicated

to

My Mother

ACKNOWLEDGEMENT

I would like to express my gratitude towards my supervisor Dr. Sanjay K. Singh for believing in my research abilities and guiding me throughout my whole research. Further, I would like to thank my PSPC committee members Dr. Biswarup Pathak and Dr. Shaikh M. Mobin for their valuable ideas and suggestions.

I also express my gratitude to Prof. Nilesh Jain, Officiating Director, IIT Indore, for his continuous support and guidance.

I extend my thanks to Dr. Biswarup Pathak (Officiating Head, Discipline of Chemistry, Indian Institute of Technology Indore) and DPGC, Dr. Tushar Kanti Mukherjee for their guidance. I am also thankful to, Dr. Satya S. Bulusu, Dr. Amrendra Kumar Singh, Dr. Anjan Chakraborty, Dr. Tridib Kumar Sharma, Dr. Tushar Kanti Mukherjee, Dr. Suman Mukhopadhyay, Dr. Apurba Kumar Das, Dr. Sampak Samanta, Dr. Biswarup Pathak, Dr. Chelvam Venkatesh and Dr. Rajneesh Misra for their guidance and help during the theoretical classes of master degree.

I am grateful to all my lab group members for their support and suggestions during my research work. I would also like to thank Ms. Anjali Bandiwadekar, Mr. Rajesh Kumar and other library staff.

I thank Mr. Kinney Pandey, Mr. Ghanshyam Bhavsar for their instrumentation support and Mr. Manish Kushwaha for assistance and technical support. Finally, I would like to express my thanks to IIT Indore for providing me an opportunity to work with advanced lab facilities to complete my masters' project.

At last but not least, I would like to express my heartiest thanks to my mother, siblings and friends for their continuous support to complete my master's project.

Chanchal Saini

ABSTRACT

In the modern era, the extensively growing global energy demand is leading to the rapid decay of fossil fuels and non-renewable energy reserves. Therefore, we need an alternative for the same. Herein, we have synthesized 2-((phenylimino) methyl)phenol **(L1),** 2-((phenylamino)methyl) phenol **(L2)**, 2-((*p*-tolylimino)methyl)phenol **(L3)** and 2-((*p*-tolylamino)methyl)phenol **(L4)**, 2-(((2,6-dimethylphenyl) imino)methyl)phenol **(L5)** and 2-(((2,6-dimethylphenyl)amino)methyl)phenol **(L6)**, 2-((mesitylimino)methyl) phenol **(L7)** and 2-((mesitylamino)methyl)phenol **(L8)** by seeking help from the literature. After successful synthesis of these ligands, corresponding arene ruthenium complexes were prepared by using [(*η6*-arene)$RuCl_2]_2$ (arene = $C_{10}H_{14}$) as an initial source of Ru. All final products were characterized by NMR and mass spectrometry. The catalytic activity of these arene-ruthenium complexes was checked for dehydrogenation of formaldehyde and formic acid at 95 °C. Using water displacement system, the volume of gas evolved was measured and TON/TOF calculated per ruthenium atom.

TABLE OF CONTENTS

LIST OF FIGURES

LIST OF TABLES

LIST OF SCHEMES

NOMENCLATURE

J	Joule
kJ	Kilo Joule
h	Hour
h^{-1}	Per hour
m	Mass
K	Kelvin
z	Charge
%	Percentage
L	Litre
g	Gram
mmol	Milli mole
mL	Milli litre
δ	Chemical shift
˚C	Degree centigrade
r.t.	Room temperature
mg	Milli gram
μL	Micro litre
ppm	Parts per million

ACRONYMS

DCM	Dichloromethane
THF	Tetrahydrofuran
KOH	Potassium hydroxide
ESI	Electrospray ionization
LCMS	Liquid chromatography-mass spectrometry
NMR	Nuclear magnetic resonance
$CDCl_3$	Chloroform-d
TON	Turnover number
TOF	Turnover frequency
H_2O	Water
TMS	Tetramethyl silane
$NaBH_4$	Sodium borohydride
Cp^*	Pentamethyl cyclopentadienyl anion
Ru	Ruthenium
HCOONa	Sodium formate
HCHO	Formaldehyde
HCOOH	Formic acid
MeOH	Methanol
CH_3OH	Methanol
LOHCs	Liquid organic hydrogen carriers
CO_2	Carbon dioxide
H_2	Dihydrogen

Chapter 1 Introduction

1.1. General Introduction:

In recent times, the booming population of the world have extensive energy demands *[1]*. In the former age, different sustainable (geothermal, wind solar and hydro energy, etc.) and non-sustainable (mainly fossil fuels) sources of energy were utilized to achieve this tremendous energy request. Massive use of fossil fuel to fulfil the energy demands of humankind led to a gradual diminish in the earth's fossil fuels reserves and also led to the explosive increase in the release of greenhouse gases leading to global warming *[2]*. So there is a need of an alternative for the fulfilment of global energy demands. Hydrogen is one of the most efficient substitute of fossil fuel for energy reserve *[3, 4]*. Because of its high enthalpy of combustion i.e. -286 kJ/mol, hydrogen can furnish considerable energy without any release of harmful gases *[4]*. In fuel cells, it can be converted to energy with water as the only by-product. Hence, can be used as a clean and dry alternative for the same *[5, 6]*.

Due to the lack of sufficient molecular hydrogen in the earth's atmosphere, there is a need for an artificial production of molecular hydrogen by various methods. Previously, production of hydrogen was done by using water-gas shift reaction and steam forming of methane at a high temperature (>200 ˚C) *[7]*. Although it's an enormous source of energy, due to its explosive nature, storage and transportation of hydrogen is not quite easy *[8-11]*. Several researchers have been working extensively to develop the novel materials like metal-organic-frame works, amine borates, carbon nanotubes, metal hydrides, doped polymers and phosphonium borates for storage and production of hydrogen *[12-14]*.

In this context, liquid organic compounds like HCHO *[15-20]*, HCOOH *[21-26]*, CH_3OH *[27]*, etc also play a major role as a hydrogen carrier, they store hydrogen in indirect form and release hydrogen at the place of need *[28]*. Formaldehyde having higher hydrogen weight efficiency 8.4 wt% than formic acid 4.4 wt% *[28,29]*. Formic acid having low

hydrogen weight efficiency but is a prominent non-toxic, biodegradable and environment-friendly organic liquid compound with easy transportation and storage *[13]*. In our work, we are focusing on catalytic dehydrogenation of both HCOOH and HCHO. Different noble metal complexes catalyze various dehydrogenation reactions of formic acid *[23]* and formaldehyde *[30]*. For dehydrogenation, the formation of metal hydride species is the key step *[28]*. Moreover, different types of ligand attached to the metal centre in a complex also tunes the activity of the complex *[29]*. Along with this, the presence of N-H moiety also enhance the activity of a catalyst, as it forms hydrogen bonding interaction with solvent or the hydrogen carrying LOC's i.e. HCOOH *[31-37]*. In the presence of catalyst formic acid decomposes to give H_2 and CO_2, whereas formaldehyde release CO_2 and two equivalent of H_2.

Dehydrogenation of formic acid was first discovered by Coffey in 1967, using Ir-phosphine complex *[38]*. In dehydrogenation of formic acid, complexes of ruthenium *[39,1,40]*, iridium *[38,41]*, palladium *[42]*, platinum *[43,44]*, and rhodium *[45,46]* transition metals have been found sufficiently active. The catalytic activity of these metal complexes has been widely investigated with fruitful results in the presence of base or additives in an aqueous system *[23]*. For instance, Pidko *et. al.* has reported TON of 706500 and TOF of 257000 h^{-1} at 90 °C using a PNP-pincer Ru-complex (PNP- 2,6-bis(di-*tert*-butyl-phosphino methyl)pyridine) in presence of amine *[47]*. Moreover, Himeda *et. al*. reported a high TON value of 14000 h^{-1} using [Cp*Ir(4,4-DHBP)(H_2O)]SO_4 as a catalyst *[7]*. In 2012, Hull *et. al.* reported TOF of 12000 h^{-1} at 60 °C for an aqueous formic acid system using Ir-bipyrimidine dimer catalyst without any base or additive, TOF can be enhanced up to 31600 h^{-1} using sodium formate as the base *[48]*. In 2014, Himeda *et. al.* reported TOF of 34000 h^{-1} at 80 °C using Ir-biimidazole complex without any base or additive *[49]*. Himeda *et. al.* has reported their improved results in 2015 after using [Cp*Ir(pyrimidylimidazoline)H_2O]SO_4 as a catalyst in an aqueous solution of HCOOH/HCOONa with a high TON value of 322000 h^{-1} *[50]*. Joo *et. al*. reported a TON of 298000 h^{-1} using an iridium-hydride

complex in formic acid dehydrogenation at 100 °C *[51]*. In 2018, Patra et.al. Reported initial TOF of 940 h^{-1} using complex $[(\eta^6\text{-}C_6H_6)Ru(\kappa^2\text{-}NpyNHMe\text{-}MAmQ)Cl]^+$ (MAmQ = 8-(Nmethylamino)quinoline and AmQ = 8-aminoquinoline) at 90 °C for formic acid dehydrogenation in presence of sodium formate *[52]*.

Along with formic acid dehydrogenation, different transition metal complexes have proven sufficiently active for dehydrogenation of formaldehyde/paraformaldehyde [30]. In the case of formaldehyde, firstly formaldehyde/paraformaldehyde catalysed to formic acid and then decompose to give H_2 and CO_2. Here, formaldehyde serves as a hydride donor and water serves as a proton donor *[15]*. As dehydrogenation of formaldehyde ($HCHO + H_2O \rightarrow 2H_2 + CO_2$) is thermodynamically favoured reaction but needs a driving force to make it kinetically favourable *[19]*. Formaldehyde dehydrogenation is a two-step process shown in scheme 1.

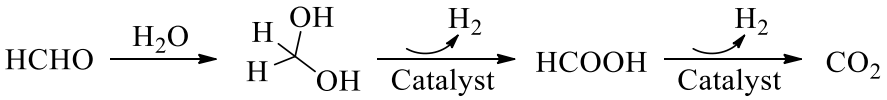

Scheme 1: Catalytic dehydrogenation of formaldehyde.

The first homogeneous catalytic system for dehydrogenation of aqueous formaldehyde reported by Prechtl et al. with a TON of 700 and initial TOF of 3142 h^{-1} at 95 °C *[15,16]*. Suenobu *et.al*. also reported a TON of 51 and an average TOF of 3.6 h^{-1} at 60 °C for H_2O/HCHO system under basic (NaOH) conditions *[17]*. Fujita et al. reported a TON of 178 under basic conditions by using [IrIII(Cp*)(6,6′-dionato-2,2′-bipyridine)-(OH)] as a catalyst *[18]*. Grutzmacher *et.al.* reported TON of 1787 and initial TOF greater than 20000 h^{-1} at 60 °C for H_2O/HCHO system under basic (KOH) conditions *[19]*.The literature data given above shows that there are so many findings by researchers, for effective dehydrogenation of formic acid as well as for formaldehyde/ paraformaldehyde. Various noble metal catalysts show high activity for the same. In concern with the conditions of the dehydrogenation, there

is a need for cost-effective catalyst that is active even at lower temperature-pressure.

1.3. Aim and Strategy of work:

Our work aims to synthesize an active Ru-arene catalyst for dehydrogenation reactions of formic acid and formaldehyde/ paraformaldehyde.

The strategy of our work is to synthesize different arene ligands using salicylaldehyde with aniline and its derivatives (scheme 2) followed by the complexation of these arene ligands with ruthenium using [(*η6*-arene)$RuCl_2]_2$ (arene = $C_{10}H_{14}$) (scheme 3).

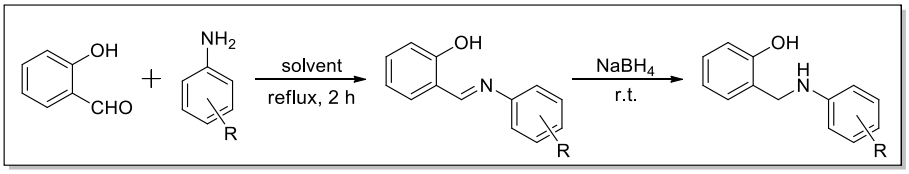

Scheme 2: Procedure for synthesis of different arene ligands.

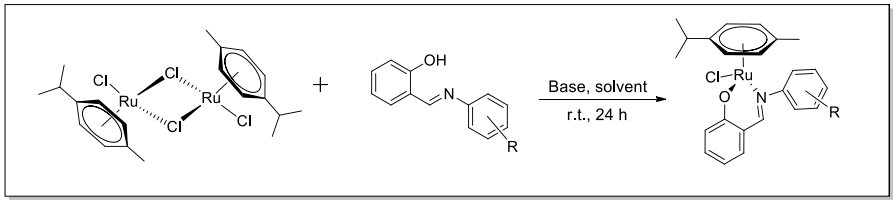

Scheme 3: Procedure for synthesis of Ru-arene complexes.

Using these Ru-arene complexes, catalytic dehydrogenation of formic acid and formaldehyde was performed at 95 ˚C and volume of evolved gas was measured by using water displacement method.

Chapter 2 Experimental Section

2.1. Materials and Instruments:

All other salts and chemicals were purchased from Merck, Alfa Aesar & Sigma-Aldrich and used without any further purification.

^{1}H NMR spectra were recorded on Bruker AVANCE 400 spectrometer using tetramethylsilane (TMS) as a reference at ambient temperature. Chemical shifts were reported in ppm relative to the centre of the singlet at 7.26 ppm for $CDCl_3$ in ^{1}H. Mass spectrometric analyses were done on Bruker-Daltonics, microTOF-Q II mass spectrometer.

2.2. Synthesis of Ligands:

2.2.1. Synthesis of L1 and L2:

L1 was synthesized by using salicylaldehyde (10 mmol, 1.066 mL) and aniline (10 mmol, 0.914 mL) in 30 mL methanol, refluxed for 2 hours. After reflux, solvent dried using rotatory vapour. We got the orange-yellow viscous liquid product (yield: 9.6 mmol, 1.720 mL, 96%). Product was characterized by mass and NMR. ^{1}H NMR (400 MHz, $CDCl_3$): δ (ppm) = 8.63 (s, 1H), 7.41 (m, 4H), 7.30 (m, 3H), 7.03 (d, 1H, *J=8* Hz), 6.95 (t, 1H, *J=8* Hz). LCMS (ESI): calculated m/z = 198.0913, observed m/z = 198.0916. Ligand (L1) (4 mmol, 0.784 g) was taken in 100 mL round bottom flask along with 20 mL methanol. Sodium borohydride (6 mmol, 0.227 g) was added to the solution and continuously stirred for 4 hours using an ice bath. After the reaction resulting solution dried and workup was done with water and DCM. Finally, the solvent was dried using rotatory vapour and we got the white solid product (yield: 3.5 mmol, 0.697 g, 87.5%). The final product (L2) was characterized by mass and NMR. ^{1}H NMR (400 MHz, $CDCl_3$): δ (ppm) = 7.20 (m, 3H), 7.13 (d, 1H, *J=4* Hz), 6.92 (m, 2H), 6.84 (m, 3H), 4.41 (s, 2H). LCMS (ESI): calculated m/z = 200.1070, observed m/z = 200.1112.

2.2.2. Synthesis of L3 and L4:

L3 was synthesized by using salicylaldehyde (10 mmol, 1.066 mL) and 4-methylaniline (10 mmol, 1.102 mL) in 30 mL methanol, refluxed for 2 hours. After reflux, solvent dried using rotatory vapour. We got the orange-yellow viscous liquid product (yield: 8.96 mmol, 1.890 mL, 89%). Product was characterized by mass and NMR. ^{1}H NMR (400 MHz, $CDCl_3$): δ (ppm) = 8.63 (s, 1H), 7.38 (d, 1H, *J=8* Hz), 7.35 (d, 1H, *J=8* Hz), 7.19 (m, 4H), 7.02 (d, 1H, *J=8* Hz), 6.94 (t, 1H, *J=8* Hz), 2.39 (s, 3H). LCMS (ESI): calculated m/z = 212.1070, observed m/z = 212.1072. Ligand (L3) (4 mmol, 0.844 g) was taken in 100 mL round bottom flask along with 20 mL methanol. Sodium borohydride (6 mmol, 0.227 g) was added to the solution and continuously stirred for 4 hours using an ice bath. After the reaction resulting solution dried and workup was done with water and DCM. Finally, the solvent was dried using rotatory vapour and we got the white solid product (yield: 3.7 mmol, 0.788 g, 92.5%). The final product (L4) was characterized by mass and NMR. ^{1}H NMR (400 MHz, $CDCl_3$): δ (ppm) = 7.21 (t, 1H, *J=8* Hz), 7.11 (d, 1H, *J=8* Hz), 7.04 (d, 2H, *J=8* Hz), 6.91 (d, 1H, *J=8* Hz), 6.85 (t, 1H, *J=8* Hz), 6.79 (d, 2H, *J=8* Hz), 4.39 (s, 2H), 2.28 (s, 3H). LCMS (ESI): calculated m/z = 214.1226, observed m/z = 214.1385.

2.2.3. Synthesis of L5 and L6:

L5 was synthesized by using salicylaldehyde (10 mmol, 1.066 mL) and 2,6-dimethylaniline (10 mmol, 1.236 mL) in 30 mL methanol, refluxed for 2 hours. After reflux, solvent dried using rotatory vapour. We got the orange-yellow viscous liquid product (yield: 8.9 mmol, 1.944 mL, 89%). Product was characterized by mass and NMR. ^{1}H NMR (400 MHz, $CDCl_3$): δ (ppm) = 8.49 (s, 1H), 7.56 (t, 1H), 7.49 (d, 1H, *J=8 Hz*), 7.26 (d, 2H, *J=8* Hz), 7.21 (d, 1H, *J=8* Hz), 7.19 (t, 1H, *J=8* Hz), 7.12 (t, 1H), 2.37 (s, 6H). LCMS (ESI): calculated m/z = 226.1226, observed m/z = 226.1234. Ligand (L5) (4 mmol, 0.900 g) was taken in 100 mL round bottom flask along with 20 mL methanol. Sodium borohydride (6 mmol, 0.227 g) was added to the solution and continuously stirred for 4

hours using an ice bath. After the reaction resulting solution dried and workup was done with water and DCM. Finally, the solvent was dried using rotatory vapour and we got the white solid product (yield: 3.4 mmol, 0.772 g, 85%). The final product (L6) was characterized by mass and NMR. ^{1}H NMR (400 MHz, $CDCl_3$): δ (ppm) = 7.25 (t, 1H, *J=8* Hz), 7.09 (t, 3H, *J=8* Hz), 7.01 (d, 1H, *J=8* Hz), 6.95 (d, 1H, *J=8* Hz), 6.86 (t, 1H, *J=8* Hz), 4.19 (s, 2H), 2.42 (s, 6H). LCMS (ESI): calculated m/z = 228.1383, observed m/z = 228.1551.

2.2.4. Synthesis of L7 and L8:

L7 was synthesized by using salicylaldehyde (10 mmol, 1.066 mL) and 2,4,6-trimethylaniline (10 mmol, 1.404 mL) in 30 mL methanol, refluxed for 2 hours. After reflux, solvent dried using rotatory vapour. We got the orange-yellow viscous liquid product (yield: 8.7 mmol, 2.038 mL, 87%). Product was characterized by mass and NMR. ^{1}H NMR (400 MHz, $CDCl_3$): δ (ppm) = 8.36 (s, 1H), 7.42 (t, 1H, *J=8* Hz), 7.35 (d, 1H, *J=8* Hz), 7.07 (d, 1H), 6.98 (t, 1H, *J=8* Hz), 6.96 (s, 2H), 2.34 (s, 3H), 2.21 (s, 6H). LCMS (ESI): calculated m/z = 240.1383, observed m/z = 240.1396. Ligand (L7) (4 mmol, 0.956 g) was taken in 100 mL round bottom flask along with 20 mL methanol. Sodium borohydride (6 mmol, 0.227 g) was added to the solution and continuously stirred for 4 hours using an ice bath. After the reaction resulting solution dried and workup was done with water and DCM. Finally, the solvent was dried using rotatory vapour and we got the white solid product (yield: 3.5 mmol, 0.844 g, 87.5%). The final product (L8) was characterized by mass and NMR. ^{1}H NMR (400 MHz, $CDCl_3$): δ (ppm) = 7.25 (t, 1H, *J=8* Hz), 7.09 (t, 3H, *J=8* Hz), 7.01 (d, 1H, *J=8* Hz), 6.95 (d, 1H, *J=8* Hz), 6.86 (t, 1H, *J=8* Hz), 4.19 (s, 2H), 2.42 (s, 6H). LCMS (ESI): calculated m/z = 242.1539, observed m/z = 242.1515.

2.3. Synthesis of Complexes:

2.3.1. Synthesis of C1:

C1 was synthesized by using [(*η6*-arene)$RuCl_2$]$_2$ (arene = $C_{10}H_{14}$) (0.2 mmol, 0.1224 g), 2-((phenylimino)methyl)phenol (L1) (0.44 mmol, 0.0867 g) and KOH (0.44 mmol, 0.0247 g) in 20 mL THF, stirred at RT for 24 hours. After the completion of the reaction, solvent dried using rotatory vapour. The crude product was dissolved in 2 mL of DCM and precipitated using petroleum ether. Precipitate washed with petroleum ether and then dried (yield: 0.3212 mmol, 0.150 g, 80.3%). Product was characterized by mass and NMR. ^{1}H NMR (400 MHz, $CDCl_3$): δ (ppm) = 7.75 (s, 1H), 7.63 (d, 2H), 7.45 (t, 2H, *J=8* Hz), 7.33 (t, 1H), 7.22 (t, 1H), 6.99 (d, 1H, *J=8* Hz), 6.94 (d, 1H, *J=8* Hz), 6.43 (t, 1H, *J=8* Hz), 5.33 (d, 1H), 5.24 (d, 1H), 4.99 (d, 1H), 4.19 (d, 1H), 2.63 (m, 1H), 2.12 (s, 3H), 1.17 (d, 3H, *J=8* Hz), 1.11 (d, 3H, *J=8* Hz). LCMS (ESI): calculated m/z = 432.0902, observed m/z = 432.0928.

2.3.2. Synthesis of C2:

C2 was synthesized by using [(*η6*-arene)$RuCl_2$]$_2$ (arene = $C_{10}H_{14}$) (0.2 mmol, 0.1224 g), 2-((*p*-tolylimino)methyl)phenol (L3) (0.44 mmol, 0.0928 g) and KOH (0.44 mmol, 0.0247 g) in 20 mL THF, stirred at RT for 24 hours. After the completion of the reaction, solvent dried using rotatory vapour. The crude product was dissolved in 2 mL of DCM and precipitated using petroleum ether. Precipitate washed with petroleum ether and then dried (yield: 0.3222 mmol, 0.155 g, 80.6%). Product was characterized by mass and NMR. ^{1}H NMR (400 MHz, $CDCl_3$): δ (ppm) = 7.73 (s, 1H), 7.51 (d, 2H), 7.21 (m, 3H), 6.98 (d, 1H, *J=8* Hz), 6.93 (d, 1H, *J=8* Hz), 6.42 (t, 1H), 5.32 (d, 1H), 5.26 (d, 1H), 4.96 (d, 1H), 4.20 (d, 1H), 2.64 (m, 1H), 2.43 (s, 3H), 2.13 (s, 3H), 1.17 (d, 3H, *J=8* Hz), 1.11 (d, 3H, *J=8* Hz). LCMS (ESI): calculated m/z = 446.1059, observed m/z = 446.1082.

2.3.3. Synthesis of C3:

C3 was synthesized by using [(*η6*-arene)$RuCl_2$]$_2$ (arene = $C_{10}H_{14}$) (0.2 mmol, 0.1224 g), 2-(((2,6-dimethylphenyl)imino)methyl)phenol (L5) (0.44 mmol, 0.0990 g) and KOH (0.44 mmol, 0.0247 g) in 20 mL THF, stirred at RT for 24 hours. After the completion of the reaction, solvent dried using rotatory vapour. The crude product was dissolved in 2 mL of DCM and precipitated using petroleum ether. Precipitate washed with petroleum ether and then dried (yield: 0.2727 mmol, 0.1350 g, 68.2%). Product was characterized by mass and NMR. ^{1}H NMR (400 MHz, $CDCl_3$): δ (ppm) = 7.42 (s, 1H), 7.16 (m, 4H), 6.93 (d, 1H, *J=8* Hz), 6.86 (d, 1H, *J=8* Hz), 6.41 (t, 1H), 5.35 (d, 1H), 5.11 (d, 1H), 4.93 (d, 1H), 4.19 (d, 1H), 2.75 (m, 1H), 2.53 (s, 3H), 2.27 (s, 3H), 1.97 (s, 3H), 1.30 (d, 3H), 1.26 (d, 3H). LCMS (ESI): calculated m/z = 460.1216, observed m/z = 460.1357.

2.3.4. Synthesis of C4:

C4 was synthesized by using [(*η6*-arene)$RuCl_2$]$_2$ (arene = $C_{10}H_{14}$) (0.2 mmol, 0.1224 g), 2-((mesitylimino)methyl)phenol (L7) (0.44 mmol, 1.0516 g) and KOH (0.44 mmol, 0.0247 g) in 20 mL THF, stirred at RT for 24 hours. After the completion of the reaction, solvent dried using rotatory vapour. The crude product was dissolved in 2 mL of DCM and precipitated using petroleum ether. Precipitate washed with petroleum ether and then dried (yield: 0.2220 mmol, 0.1130 g, 55.5%). Product was characterized by mass and NMR. ^{1}H NMR (400 MHz, $CDCl_3$): δ (ppm) = 7.40 (s, 1H), 7.17 (t, 1H, *J=8* Hz), 7.02 (s, 1H), 6.99 (s, 1H), 6.92 (d, 1H, *J=8* Hz), 6.85 (d, 1H, *J=8* Hz), 6.40 (t, 1H, *J=8* Hz), 5.36 (d, 1H), 5.14 (d, 1H), 4.91 (d, 1H), 4.20 (d, 1H), 2.77 (m, 1H), 2.52 (s, 3H), 2.37 (s, 3H), 2.22 (s, 3H), 1.99 (s, 3H), 1.31 (d, 3H), 1.26 (d, 3H). LCMS (ESI): calculated m/z = 474.1372, observed m/z = 474.1134.

2.4. General procedure for the catalytic dehydrogenation of aqueous formaldehyde using different Ru-arene complexes:

37 wt% aq. formaldehyde (13.55 mmol, 1.016 mL) was dehydrogenated in 4 mL two necked tube. C1, C2, C3 and C4 were used as a catalyst

(0.1 mol %, 0.013 mmol) and the reaction mixture was heated at 95 °C as shown in scheme 4.

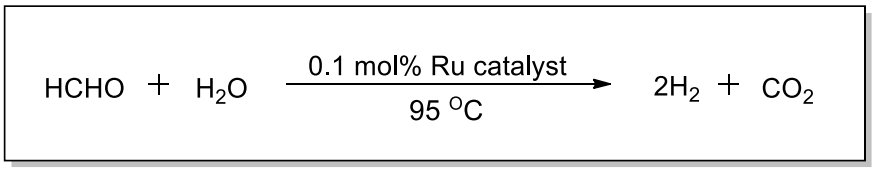

Scheme 4: General procedure for the catalytic dehydrogenation of aq. formaldehyde using Ru-arene complex.

The volume of evolved gas was measured by water displacement method. Turn over number (TON) and turn over frequency (TOF) values were calculated by using formula given below:

$$\text{mmol of gas evolved} = \frac{\text{mL of gas evolved}}{24.5\ \text{mL/mmol}}$$

$$\text{TON} = \frac{\text{mmol of gas evolved}}{\text{mmol of catalyst}}$$

$$\text{TOF} = \frac{\text{TON}}{\text{time taken (h)}}$$

By following the same procedure, dehydrogenation of formaldehyde was done by using all Ru-arene complexes i.e. C1, C2, C3 and C4.

2.5. General procedure for the catalytic dehydrogenation of formic acid using Ru-arene complex:

Formic acid (10 mmol, 378 μL) was dehydrogenated in 25 mL round bottom flask (RB). Previously synthesized Ru-arene complex **C1** was used as a catalyst (0.01 mmol, 4.68 mg) in 5 mL aqueous solution and reaction mixture was heated at 95 °C as shown in scheme 5.

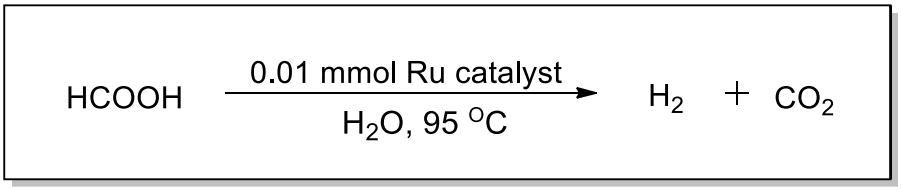

Scheme 5: General procedure for the catalytic dehydrogenation of formic acid using Ru-arene complex **C1**.

The volume of evolved gas was measured by water displacement method. Turn over number (TON) and turn over frequency (TOF) values were calculated by using given formula:

$$\text{TON} = \frac{\text{mmol of gas evolved}}{\text{mmol of catalyst}}$$

$$\text{TOF} = \frac{\text{TON}}{\text{time taken (h)}}$$

Chapter 3 Results and discussion

3.1. Synthesis and characterization of ligands:

Ligand **L1** was synthesized by refluxing salicylaldehyde with aniline as shown in scheme 6. We got a viscous product with 96% yield (9.6 mmol, 1.720 mL). The obtained product was characterized by using ^{1}H NMR and mass spectrometry.

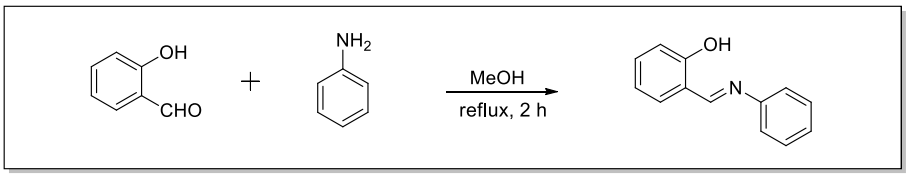

Scheme 6: Synthesis of ligand L1.

LCMS of L1 (figure 1) showing that we got a signal m/z equals to 198.0916, where m = M + 1 and z = 1. Along with the intense signal, there is an isotopic weak signal at m/z = 199.0933 due to the presence of isotope of hydrogen. Calculated m/z = 198.0913 and observed m/z = 198.0916.

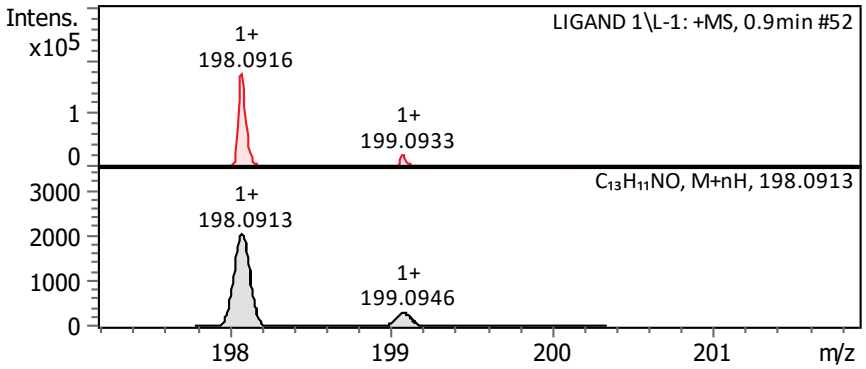

Figure 1: Mass spectrogram of ligand L1.

Figure 2 showing the ^{1}H NMR spectrum of L1, here we observed the solvent peak (chloroform-d) at 7.26 ppm and a singlet for 1 hydrogen at 8.63 ppm that corresponds to the characteristic peak of imine. Peaks for 9 aromatic hydrogens are observed in the range 7.5-6.9 ppm.

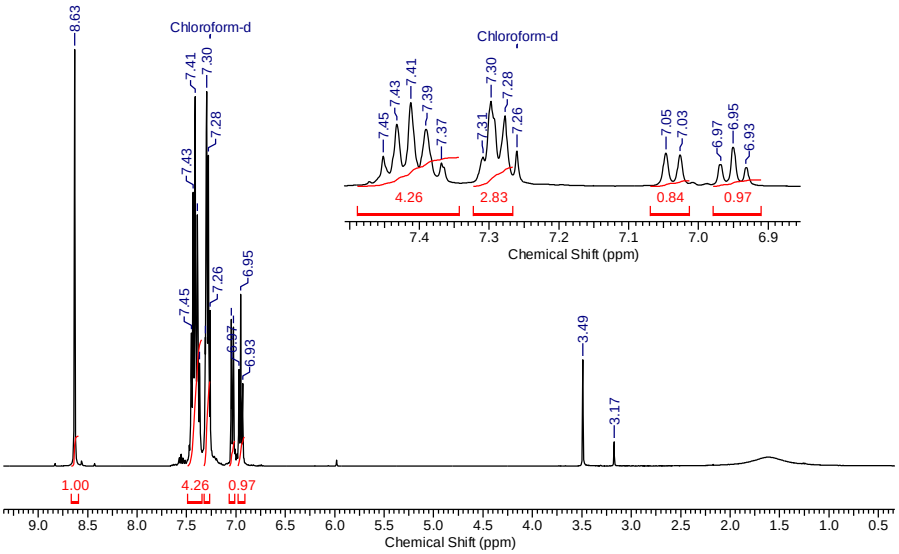

Figure 2: ^{1}H NMR spectrum of L1.

Ligand **L2** was synthesized by reduction of ligand **L1** using $NaBH_4$ at 0 ˚C as shown in scheme 7. We got a solid white product with 88% yield (3.5 mmol, 0.697 g). The obtained product was characterized by using ^{1}H NMR and mass spectrometry.

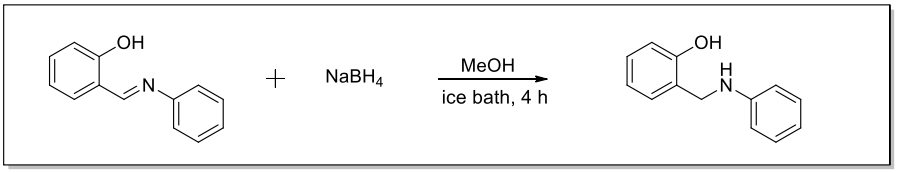

Scheme 7: Synthesis of ligand L2.

LCMS of L2 (figure 3) showing that we got a signal m/z equals to 200.1112, where m = M + 1 and z = 1. Along with the intense signal, there is an isotopic weak signal at m/z = 201.1122 due to the presence of isotope of hydrogen. Calculated m/z = 200.1070 and observed m/z = 200.1112.

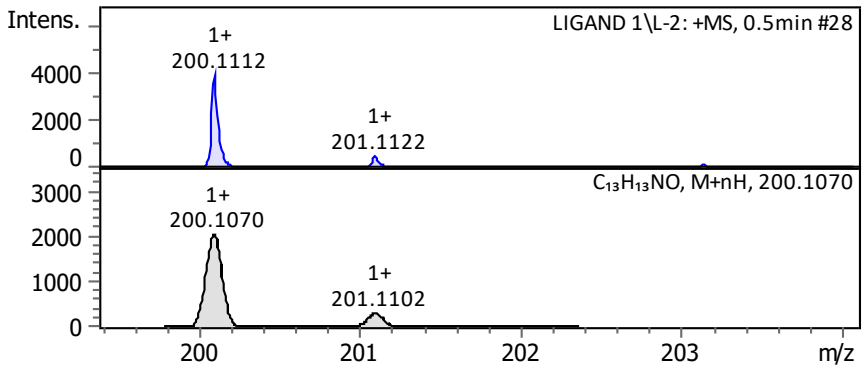

Figure 3: Mass spectrogram of ligand L2.

Figure 4 showing the ^{1}H NMR spectrum of L2, here we observed the solvent peak (chloroform-d) at 7.26 ppm. Peaks for 9 aromatic hydrogens are observed in the range 7.3-6.8 ppm. A singlet for 2 hydrogens at 4.41 ppm that corresponds to the hydrogens of -CH_2-.

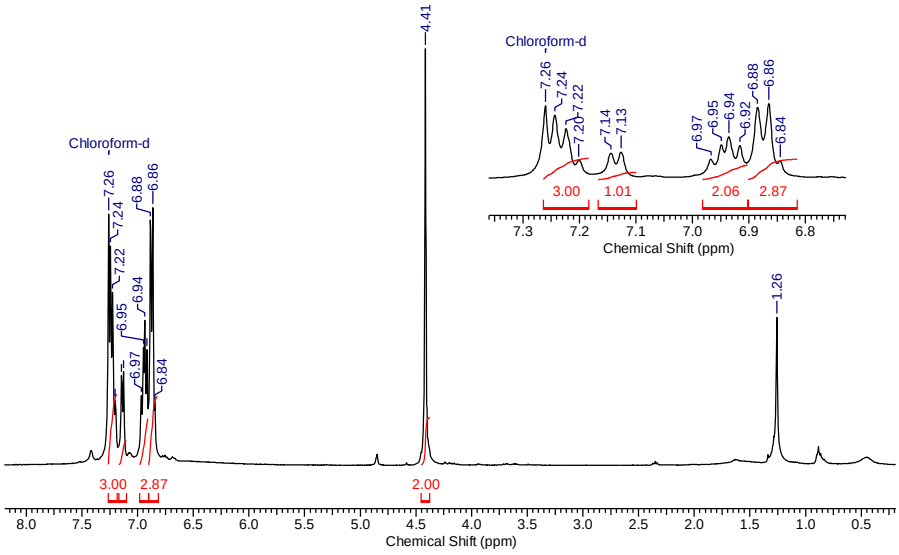

Figure 4: ^{1}H NMR spectrum of L2.

Ligand **L3** was synthesized by refluxing salicylaldehyde with 4-methylaniline as shown in scheme 8. We got a viscous product with 89% yield (8.96 mmol, 1.890 mL). The obtained product was characterized by using ^{1}H NMR and mass spectrometry.

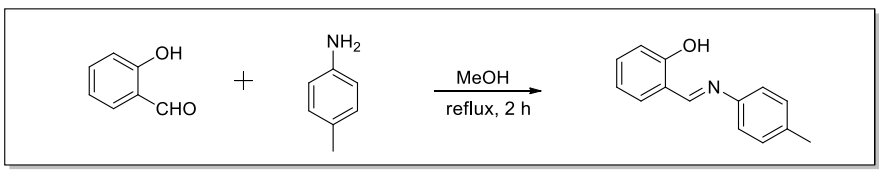

Scheme 8: Synthesis of ligand L3.

LCMS of L3 (figure 5) showing that we got a signal m/z equals to 212.1072, where m = M + 1 and z = 1. Along with the intense signal, there is an isotopic weak signal at m/z = 213.1097 due to the presence of isotope of hydrogen. Calculated m/z = 212.1070 and observed m/z = 212.1072.

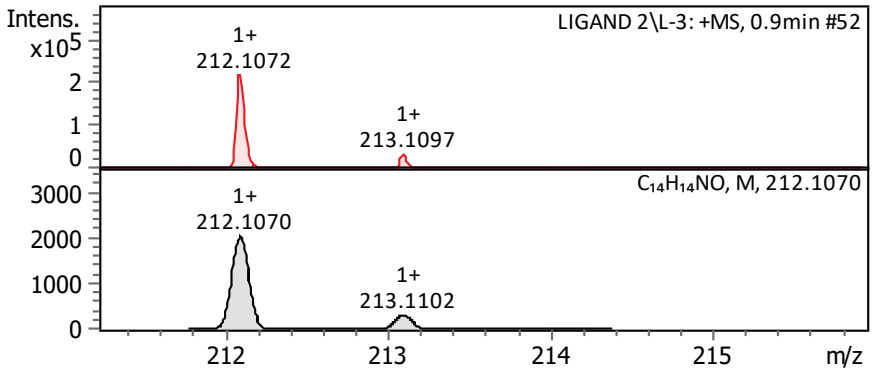

Figure 5: Mass spectrogram of ligand L3.

Figure 6 showing the ^{1}H NMR spectrum of L3, here we observed the solvent peak (chloroform-d) at 7.26 ppm and a singlet for 1 hydrogen at 8.63 ppm that corresponds to the characteristic peak of imine. Peaks for 8 aromatic hydrogens are observed in the range 7.5-6.9 ppm and a singlet for 3 hydrogens at 2.39 ppm shows the presence of -CH_3 in the phenyl ring.

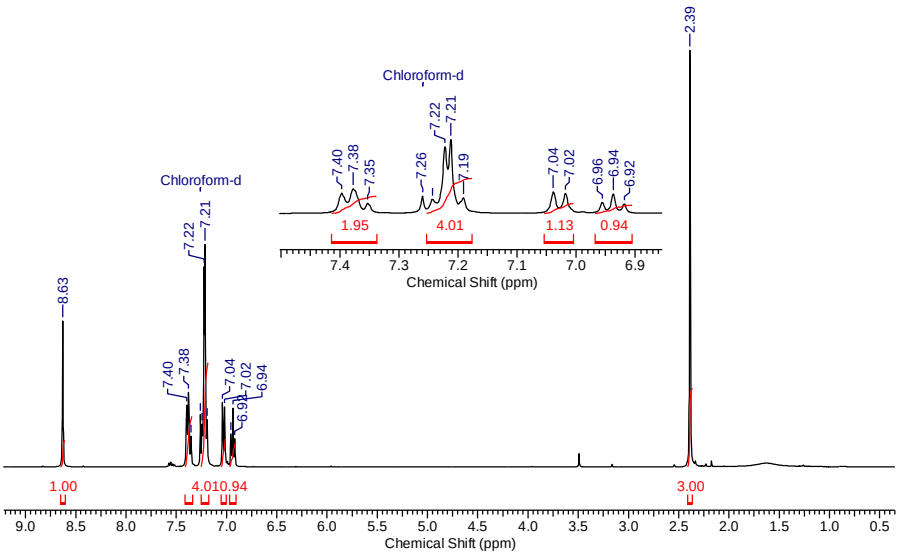

Figure 6: ^{1}H NMR spectrum of L3.

Ligand **L4** was synthesized by reduction of ligand **L3** using $NaBH_4$ at 0 °C as shown in scheme 9. We got a solid white product with a 93% yield (3.7 mmol, 0.788 g). The obtained product was characterized by using ^1H NMR and mass spectrometry.

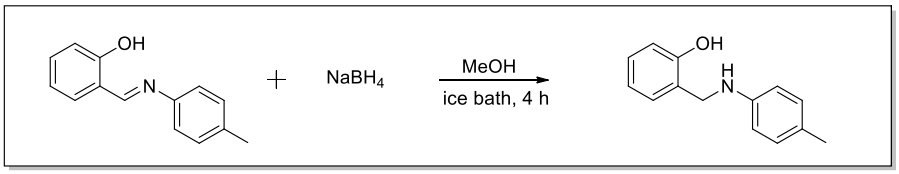

Scheme 9: Synthesis of ligand L4.

LCMS of L4 (figure 7) showing that we got a signal m/z equals to 214.1385, where m = M + 1 and z = 1. Along with the intensed signal there is an isotopic weak signal at m/z = 215.1423 due to the presence of isotope of hydrogen. Calculated m/z = 214.1226 and observed m/z = 214.1385.

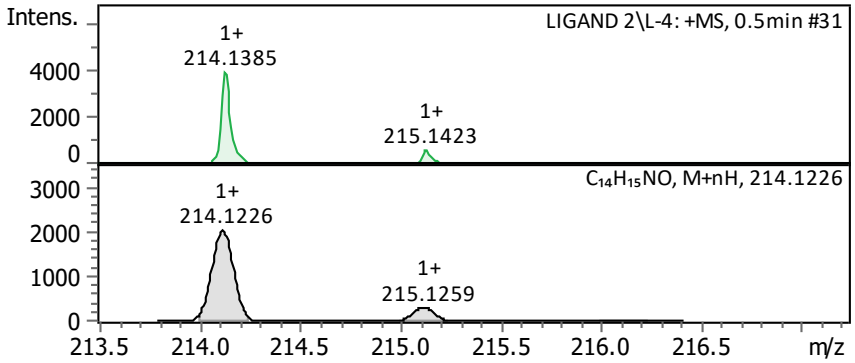

Figure 7: Mass spectrogram of ligand L4.

Figure 8 showing the ^1H NMR spectrum of L4, here we observed the solvent peak (chloroform-d) at 7.26 ppm and peaks for the 8 aromatic hydrogens observed in the range 7.25-6.79 ppm. A singlet for 2 hydrogens at 4.39 ppm that corresponds to the hydrogens of $-CH_2-$ while a singlet for 3 hydrogens at 2.28 ppm represents the presence of $–CH_3$ at the para position of the phenyl ring.

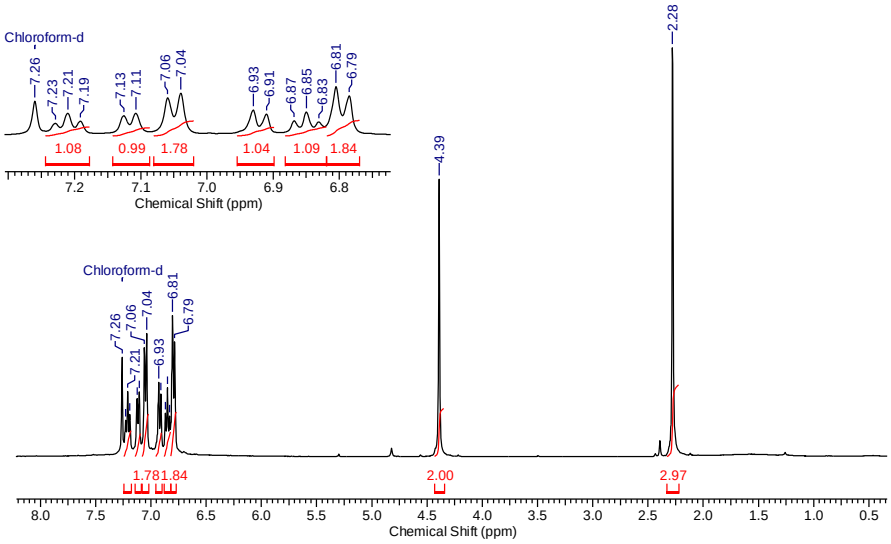

Figure 8: ^{1}H NMR spectrum of L4.

Ligand **L5** was synthesized by refluxing salicylaldehyde with 2, 6-dimethylaniline as shown in scheme 10. We got a viscous product with an 89% yield (8.9 mmol, 1.944 mL). The obtained product was characterized by using ^{1}H NMR and mass spectrometry.

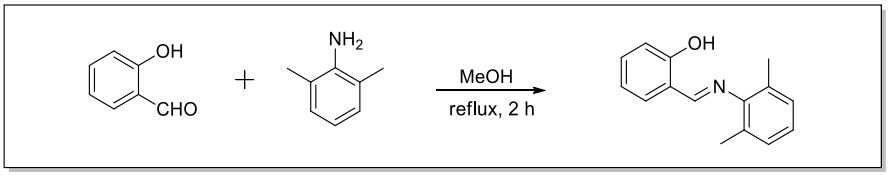

Scheme 10: Synthesis of ligand L5.

LCMS of L5 (figure 9) showing that we got a signal m/z equals to 226.1234, where m = M + 1 and z = 1. Along with the intense signal, there is an isotopic weak signal at m/z = 227.1257 due to the presence of isotope of hydrogen. Calculated m/z = 226.1226 and observed m/z = 226.1234.

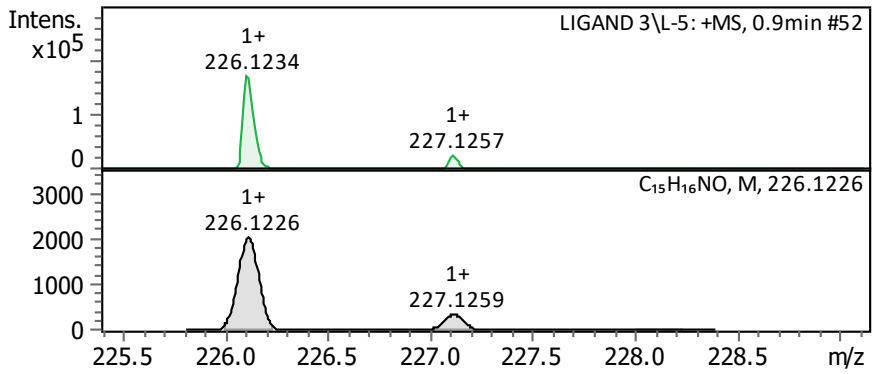

Figure 9: Mass spectrogram of ligand L5.

Figure 10 showing the ^{1}H NMR spectrum of L5, here we observed the solvent peak (chloroform-d) at 7.26 ppm and a singlet for 1 hydrogen at 8.49 ppm that corresponds to the characteristic peak of imine. Peaks for 7 aromatic hydrogens are observed in the range 7.58-7.10 ppm and a singlet for 6 hydrogens at 2.37 ppm shows the presence of two -CH_3 in the phenyl ring.

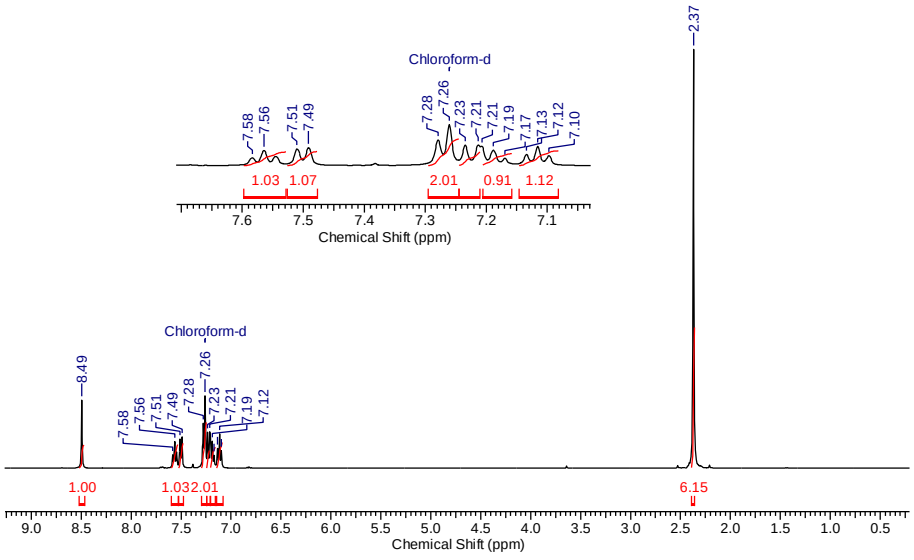

Figure 10: ^{1}H NMR spectrum of L5.

Ligand **L6** was synthesized by reduction of ligand **L$_5$** using $NaBH_4$ at 0 ˚C as shown in scheme 11. We got a solid white product with an 85% yield (3.4 mmol, 0.772 g). The obtained product was characterized by using ^{1}H NMR and mass spectrometry.

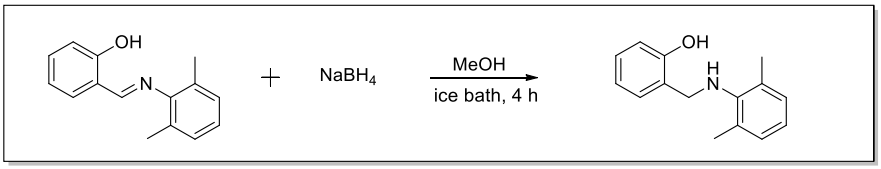

Scheme 11: Synthesis of ligand L6.

LCMS of L6 (figure 11) showing that we got a signal m/z equals to 228.1551, where m = M + 1 and z = 1. Along with the intense signal, there is an isotopic weak signal at m/z = 229.1568 due to the presence of isotope of hydrogen. Calculated m/z = 228.1383 and observed m/z = 228.1551.

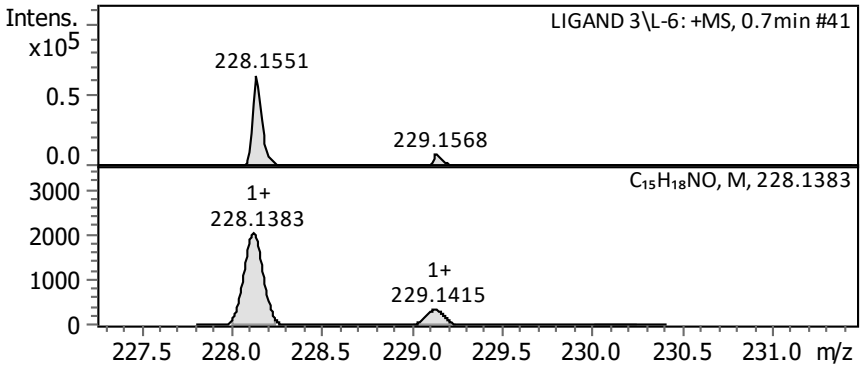

Figure 11: Mass spectrogram of ligand L6.

Figure 12 showing the ^{1}H NMR spectrum of L6, here we observed the solvent peak (chloroform-d) at 7.26 ppm and peaks for the 7 aromatic hydrogens observed in the range 7.27-6.84 ppm. A singlet for 2 hydrogens at 4.19 ppm that corresponds to the hydrogens of -CH_2- while a singlet for 6 hydrogens at 2.42 ppm represents the presence of two -CH_3 at the ortho positions of the phenyl ring.

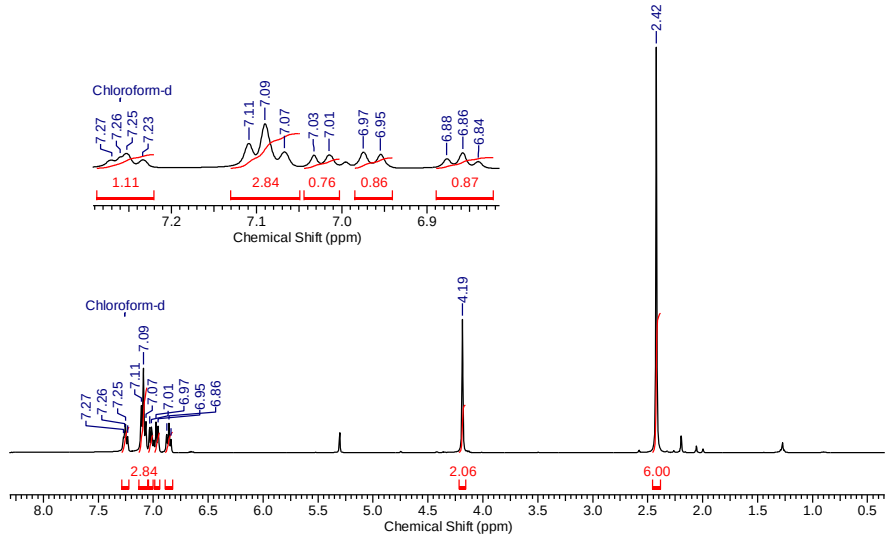

Figure 12: ^{1}H NMR spectrum of L6.

Ligand **L7** was synthesized by refluxing salicylaldehyde with 2, 4, 6-trimethylaniline as shown in scheme 12. We got a viscous product with an 87% yield (8.7 mmol, 2.038 mL). The obtained product was characterized by using ^{1}H NMR and mass spectrometry.

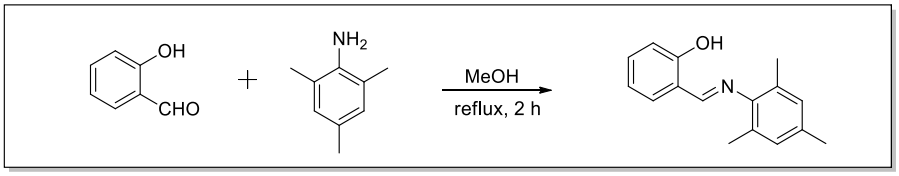

Scheme 12: Synthesis of ligand L7.

LCMS of L7 (figure 13) showing that we got a signal m/z equals to 240.1396, where m = M + 1 and z = 1. Along with the intense signal, there is an isotopic weak signal at m/z = 241.1424 due to the presence of isotope of hydrogen. Calculated m/z = 240.1383 and observed m/z = 240.1396.

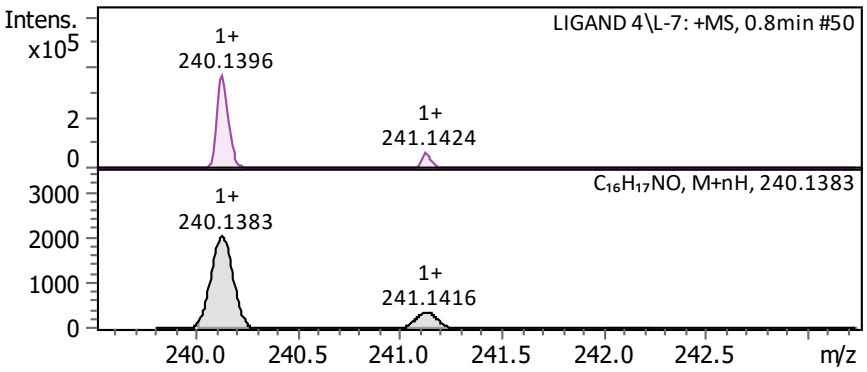

Figure 13: Mass spectrogram of ligand L7.

Figure 14 showing the ^{1}H NMR spectrum of L7, here we observed the solvent peak (chloroform-d) at 7.26 ppm and a singlet for 1 hydrogen at 8.36 ppm that corresponds to the characteristic peak of imine. Peaks for 6 aromatic hydrogens are observed in the range 7.44 6.96 ppm. Singlet for 3 hydrogens at 2.34 ppm shows the presence of $-CH_3$ at the para position while singlet for 6 hydrogens at 2.21 ppm shows the presence of the two $-CH_3$ at ortho positions in the phenyl ring.

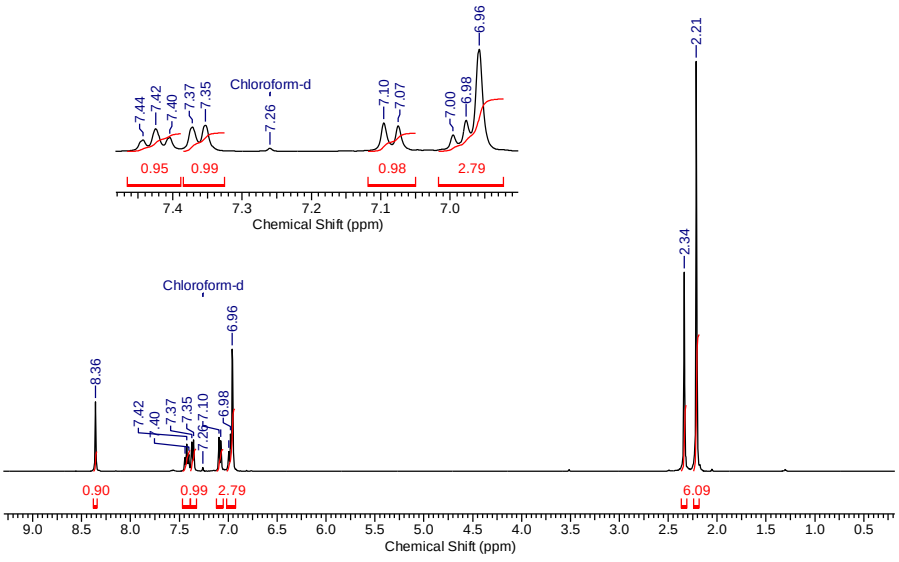

Figure 14: ^{1}H NMR spectrum of L7.

Ligand **L8** was synthesized by reduction of ligand **L7** using $NaBH_4$ at 0 ˚C as shown in scheme 13. We got a solid white product with an 88% yield (3.5 mmol, 0.884 g). The obtained product was characterized by using ^{1}H NMR and mass spectrometry.

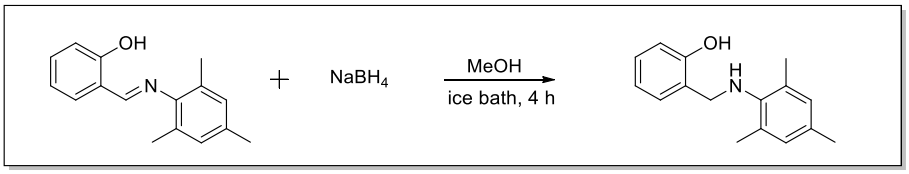

Scheme 13: Synthesis of ligand L8.

LCMS of L8 (figure 15) showing that we got a signal m/z equals to 242.1515, where m = M + 1 and z = 1. Along with the intense signal, there is an isotopic weak signal at m/z = 243.1550 due to the presence of isotope of hydrogen. Calculated m/z = 242.1539 and observed m/z = 242.1515.

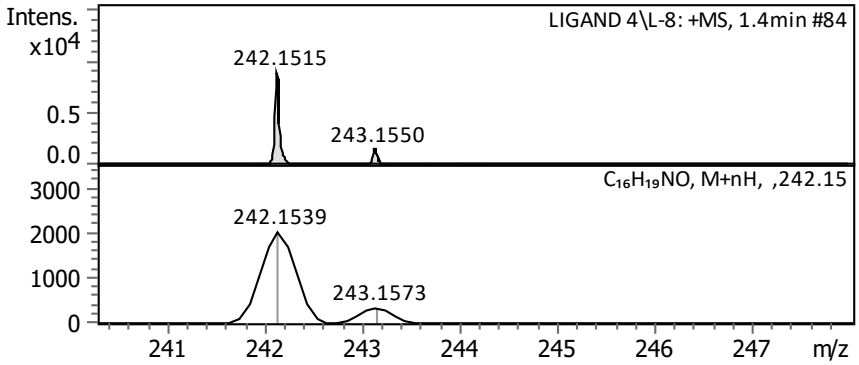

Figure 15: Mass spectrogram of ligand L8.

Figure 16 showing the ^{1}H NMR spectrum of L8, here we observed the solvent peak (chloroform-d) at 7.26 ppm and peaks for the aromatic hydrogens observed in the range 7.26-6.83 ppm. A singlet for 2 hydrogens at 4.15 ppm that corresponds to the hydrogens of -CH_2- while a singlet for 6 hydrogens at 2.38 ppm represents the presence of two -CH_3 at the ortho positions and another singlet for 3 hydrogens at 2.28 ppm represents the presence of -CH_3 at the para position of the phenyl ring.

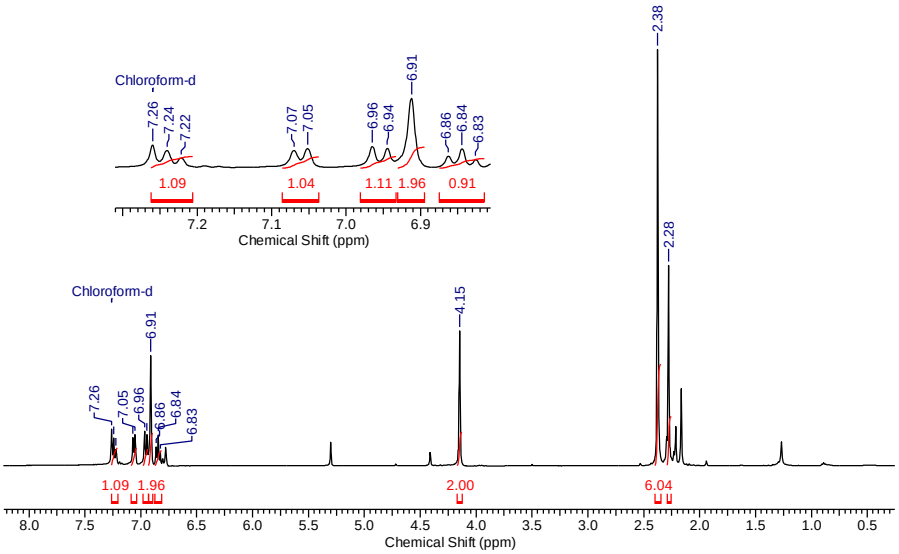

Figure 16: ^{1}H NMR spectrum of L8.

3.2. Synthesis and characterization of complexes:

Complex **C1** was synthesized by using [(η6-arene)$RuCl_2$]$_2$ (arene = $C_{10}H_{14}$) with ligand **(L1)** 2-((phenylimino)methyl)phenol in the presence of a base as shown in Scheme 14. We got a red crystalline solid product with an 80 % yield (0.3212 mmol, 0.150 g). The obtained product was characterized by using ^{1}H NMR and mass spectrometry.

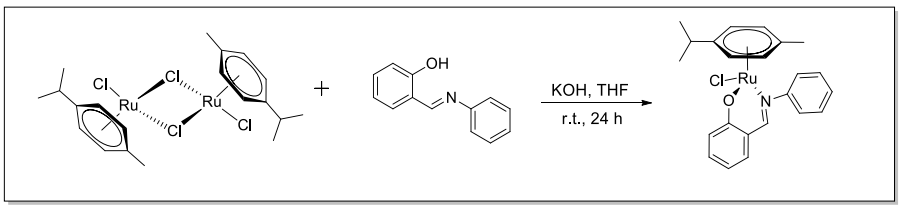

Scheme 14: Synthesis of Complex C1.

LCMS of C1 (figure 18) showing that we got a signal m/z equals to 432.0928, where m = M^+ and z = 1. The given spectrogram is for the cationic species of complex 1 shown in figure 17. Along with the intense signal, there are some weak isotopic signals on both sides of the major peak due to the presence of isotope of ruthenium. Calculated m/z = 432.0902 and observed m/z = 432.0928.

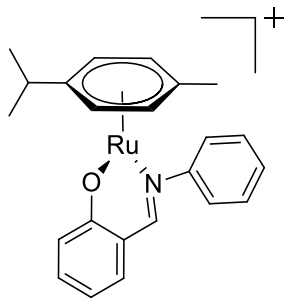

Figure 17: Cationic species of Complex C1.

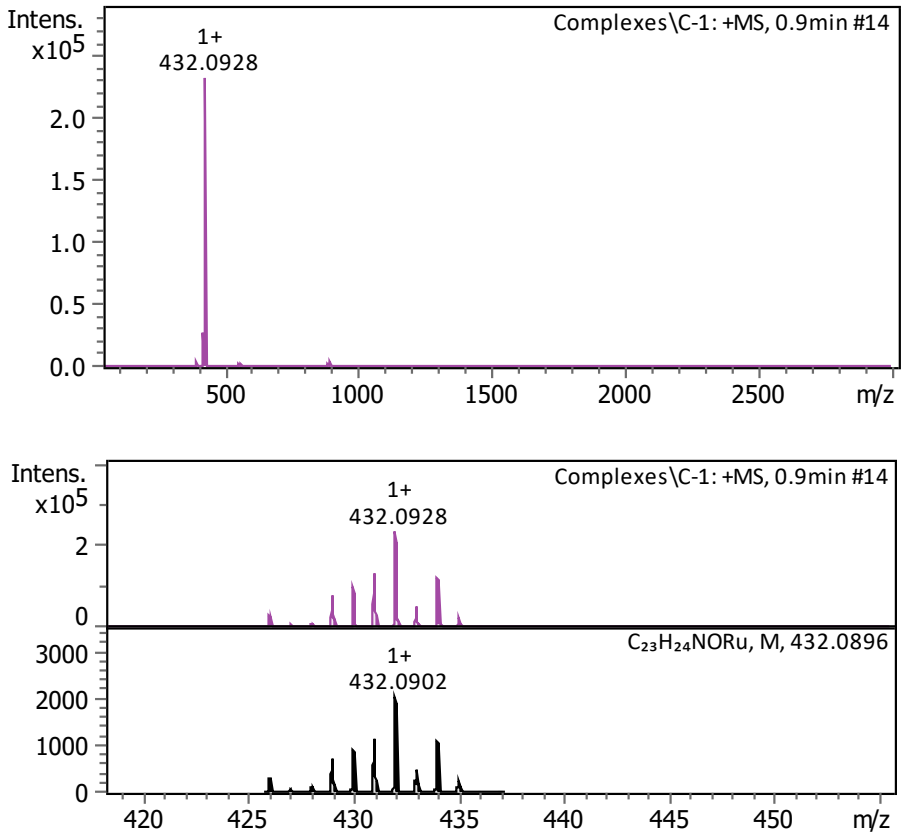

Figure 18: Mass spectrogram of Complex C1.

Figure 19 showing the ^{1}H NMR spectrum of C1, here we observed the solvent peak (chloroform-d) at 7.26 ppm and a singlet for 1 hydrogen at 7.75 ppm that corresponds to the characteristic peak of imine of the ligand. Peaks for 9 aromatic hydrogens of the ligand are observed in the range 7.65-6.94 ppm. Doublets at 5.35, 5.26, 5.00, 4.21 ppm represent the 4 aromatic hydrogens of the ring while a multiplet at 2.66 ppm is for the tertiary hydrogen of the para-cymene. Doublets at 1.19, 1.13 ppm are for the two -CH_3 at tertiary carbon and a singlet at 2.12 ppm is for -

CH_3 at the para position of the para-cymene ring. Here, we can see that there is a shift in characteristic peak of imine of the ligand. In free ligand, the singlet for 1H of imine is observed at 8.63 ppm while in complex the same singlet is observed at 7.75 ppm. This variation in chemical shift is due to increase in electron density near H of imine.

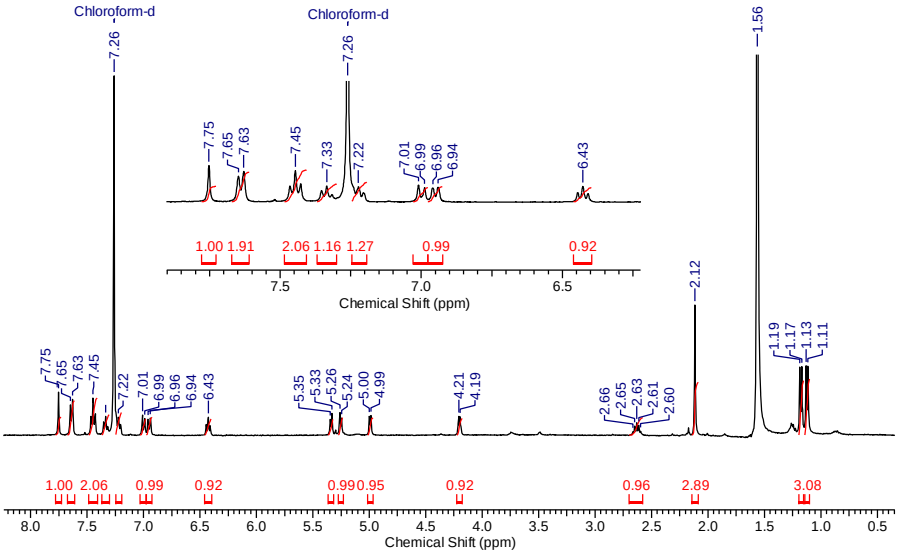

Figure 19: ^{1}H NMR spectrum of Complex C1.

Complex **C2** was synthesized by using $[(\eta 6\text{-arene})RuCl_2]_2$ (arene = $C_{10}H_{14}$) with ligand **(L3)** 2-((*p*-tolylimino)methyl)phenol in the presence of a base as shown in Scheme 15. We got a red crystalline solid product with an 81% yield (0.3222 mmol, 0.155 g). The obtained product was characterized by using ^{1}H NMR and mass spectrometry.

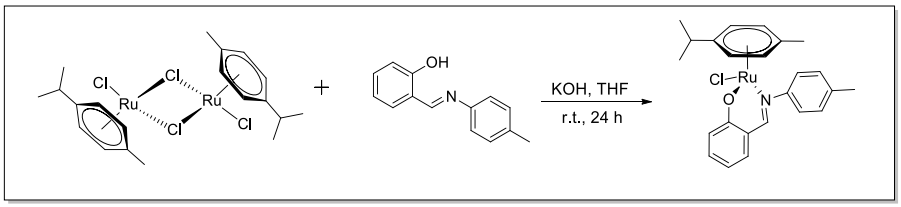

Scheme 15: Synthesis of Complex C2.

LCMS of C2 (figure 21) showing that we got a signal m/z equals to 446.1082, where m = M^+ and z = 1. The given spectrogram is for the cationic species of complex 2 shown in figure 20. Along with the intense signal, there are some weak isotopic signals on both sides of the major

peak due to the presence of isotope of ruthenium. Calculated m/z = 446.1059 and observed m/z = 446.1082.

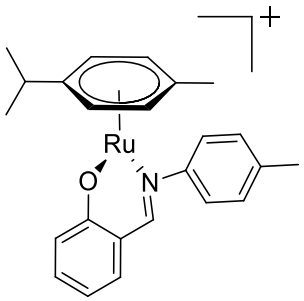

Figure 20: Cationic species of Complex C2.

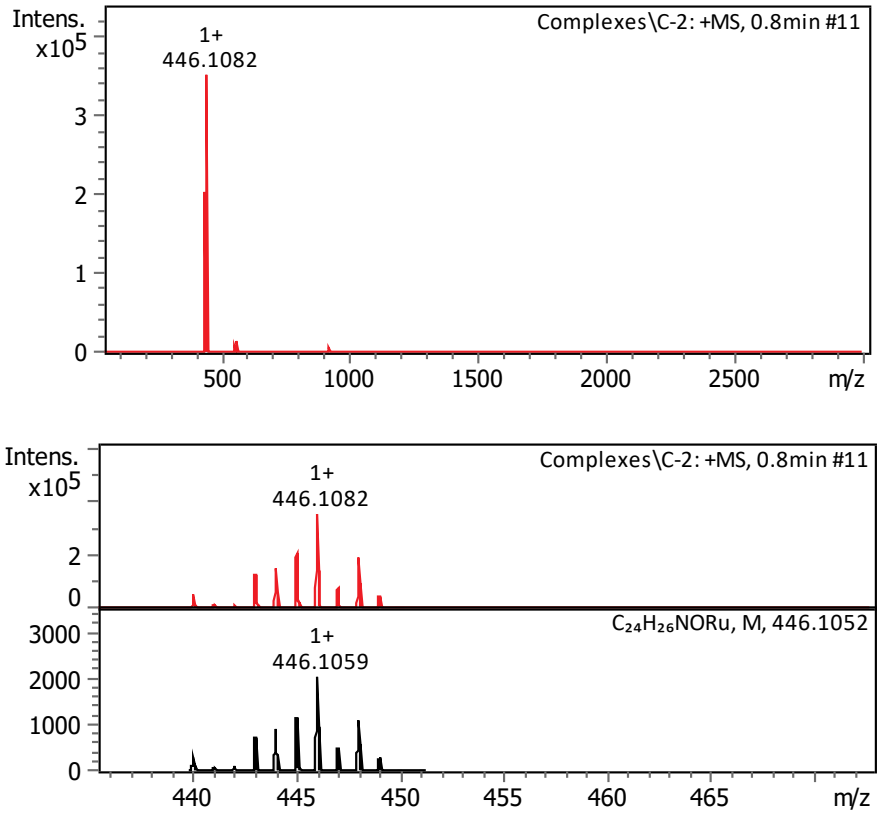

Figure 21: Mass spectrogram of Complex C2.

Figure 22 showing the ^{1}H NMR spectrum of C2, here we observed the solvent peak (chloroform-d) at 7.26 ppm and a singlet for 1 hydrogen at 7.73 ppm that corresponds to the characteristic peak of imine of the ligand. Peaks for 8 aromatic hydrogens of the ligand are observed in the range 7.53-6.40 ppm. Singlet for 3 hydrogens at 2.43 ppm shows the presence of the -CH_3 at the para position of the phenyl ring in the ligand.

Doublets at 5.34, 5.27, 4.97, 4.22 ppm represent the 4 aromatic hydrogens of the ring while a multiplet at 2.68 ppm is for the tertiary hydrogen of the para-cymene. Doublets at 1.19, 1.12 ppm are for the two -CH_3 at tertiary carbon and a singlet at 2.13 ppm shows the -CH_3 at the para position of the para-cymene ring respectively. Here, we can see that there is a shift in characteristic peak of imine of the ligand. In free ligand, the singlet for 1H of imine is observed at 8.63 ppm while in complex the same singlet is observed at 7.73 ppm. This variation in chemical shift is due to increase in electron density near H of imine.

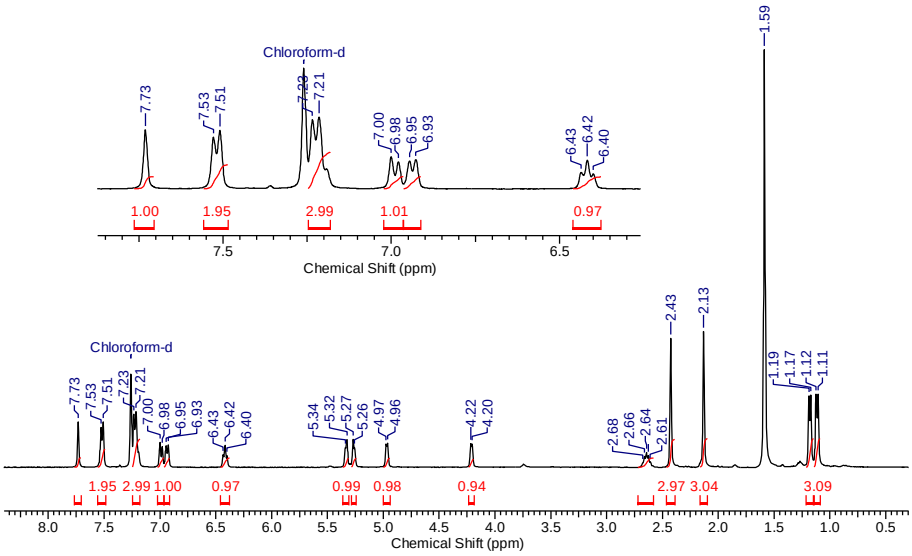

Figure 22: ^{1}H NMR spectrum of Complex C2.

Complex **C3** was synthesized by using dichloro(*p*-cymene)Ru(II) dimer with ligand **(L5)** 2-(((2,6-dimethylphenyl)imino)methyl)phenol in presence of a base as shown in Scheme 16. We got a red crystalline solid product with 68% yield (0.2727 mmol, 0.1350 g). The obtained product was characterized by using ^{1}H NMR and mass spectrometry.

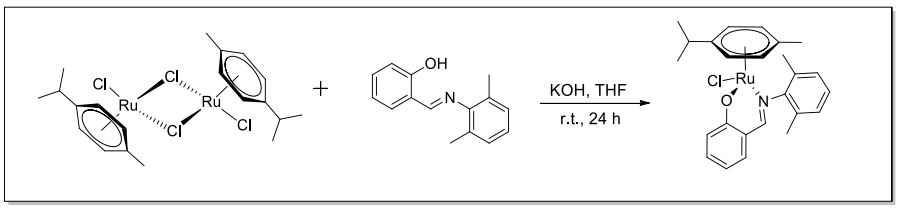

Scheme 16: Synthesis of Complex C3.

LCMS of C3 (figure 24) showing that we got a signal m/z equals to 460.1357, where m = M^+ and z = 1. The given spectrogram is for the cationic species of complex 3 shown in figure 23. Along with the intense signal, there are some weak isotopic signals on both sides of the major peak due to the presence of isotope of ruthenium. Calculated m/z = 460.1216 and observed m/z = 460.1357.

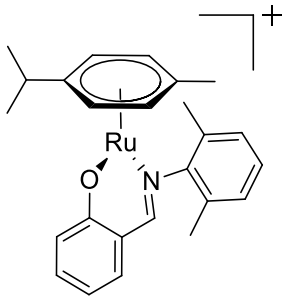

Figure 23: Cationic species of Complex C3.

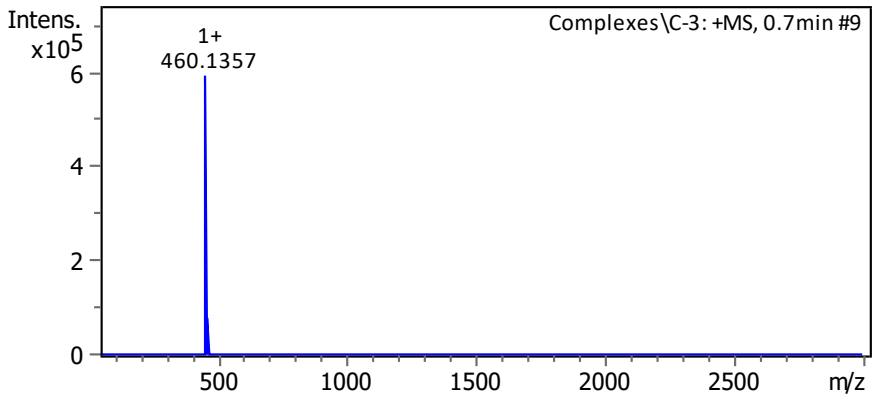

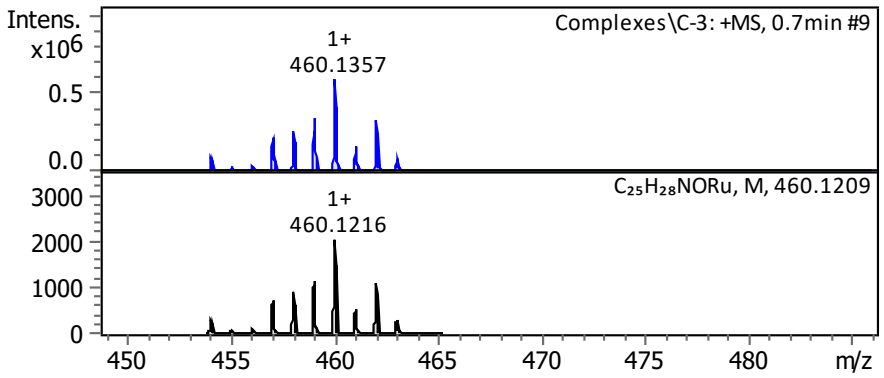

Figure 24: Mass spectrogram of Complex C3.

Figure 25 showing the ^{1}H NMR spectrum of C3, here we observed the solvent peak (chloroform-d) at 7.26 ppm and a singlet for 1 hydrogen at 7.42 ppm that corresponds to the characteristic peak of imine of the ligand. Peaks for 7 aromatic hydrogens of the ligand are observed in the range 7.20-6.40 ppm. Singlets for 3 hydrogens at 2.57 ppm and 2.27 ppm shows the presence of two different -CH_3 at the ortho positions of the phenyl ring in the ligand. Doublets at 5.37, 5.13, 4.95, 4.20 ppm represent the 4 aromatic hydrogens of the ring while a multiplet at 2.78 ppm is for the tertiary hydrogen of the para-cymene. Doublets at 1.28, 1.26 ppm are for the two -CH_3 at tertiary carbon and a singlet at 1.97 ppm shows the -CH_3 at the para position of the para-cymene ring respectively. Here, we can see that there is a shift in characteristic peak of imine of the ligand. In free ligand, the singlet for 1H of imine is observed at 8.49 ppm while in complex the same singlet is observed at 7.42 ppm. This variation in chemical shift is due to increase in electron density near H of imine.

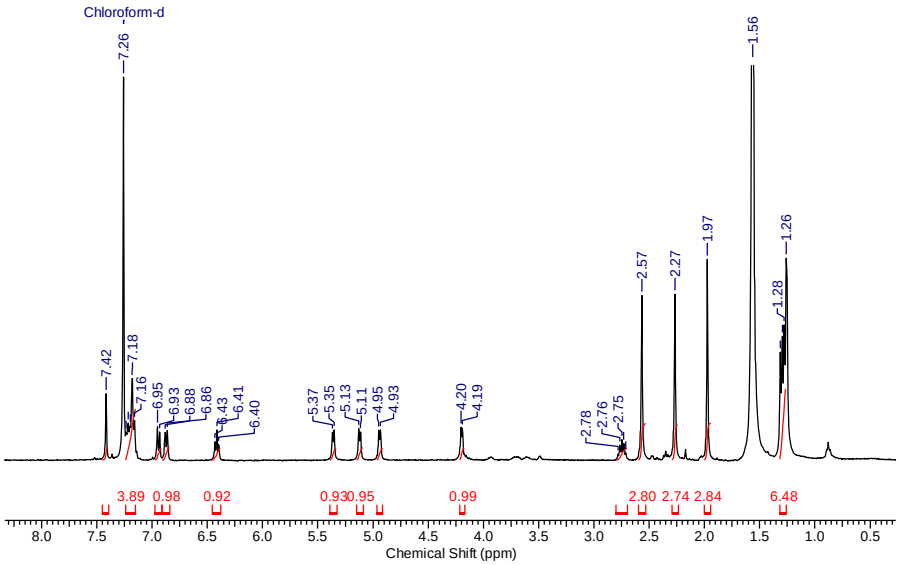

Figure 25: ^{1}H NMR spectrum of Complex C3.

Complex **C4** was synthesized by using dichloro(*p*-cymene)Ru(II) dimer with ligand **(L7)** 2-((mesitylimino)methyl)phenol in the presence of a base as shown in Scheme 17. We got a red crystalline solid product with 56% yield (0.2220 mmol, 0.1130 g). The obtained product was characterized by using ^{1}H NMR and mass spectrometry.

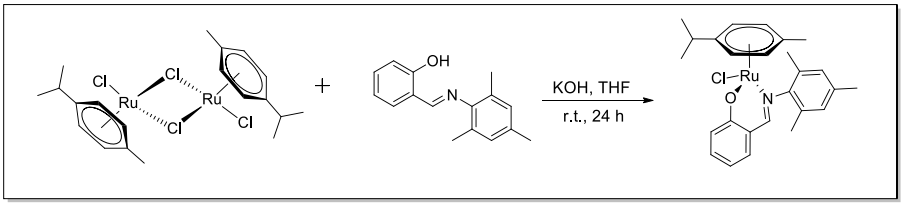

Scheme 17: Synthesis of Complex C4.

LCMS of C4 (figure 27) showing that we got a signal m/z equals to 474.1134, where m = M^{+} and z = 1. The given spectrogram is for the cationic species of complex 4 shown in figure 26. Along with the intense signal, there are some weak isotopic signals on both sides of the major peak due to the presence of isotope of ruthenium. Calculated m/z = 474.1372 and observed m/z = 474.1134.

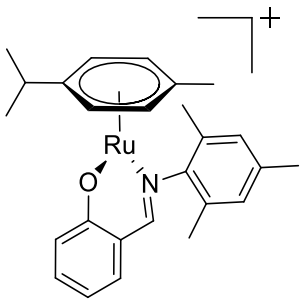

Figure 26: Cationic species of Complex C4.

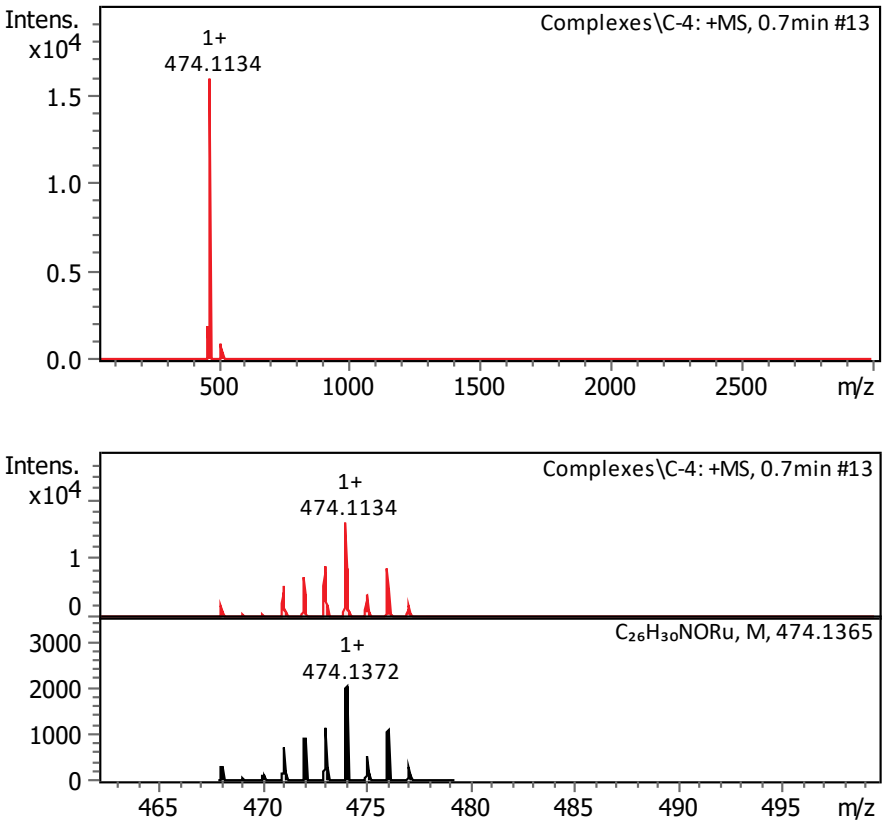

Figure 27: Mass spectrogram of Complex C4.

Figure 28 showing the ^{1}H NMR spectrum of C4, here we observed the solvent peak (chloroform-d) at 7.26 ppm and a singlet for 1 hydrogen at 7.40 ppm that corresponds to the characteristic peak of imine of the ligand. Peaks for 6 aromatic hydrogens of the ligand are observed in the range 7.20-6.38 ppm. Singlets for 3 hydrogens at 2.52, 2.37 and 2.22 ppm were observed for the three different -CH_3 at the ortho and para positions of the phenyl ring in the ligand. Doublets at 5.37, 5.16, 4.93, 4.21 ppm represent the 4 aromatic hydrogens of the ring while a

multiplet at 2.80 ppm is for the tertiary hydrogen of the para-cymene. Doublets at 1.33, 1.27 ppm are for the two -CH_3 at tertiary carbon and a singlet at 1.99 ppm shows the -CH_3 at the para position of the para-cymene ring respectively. Here, we can see that there is a shift in characteristic peak of imine of the ligand. In free ligand, the singlet for 1H of imine is observed at 8.36 ppm while in complex the same singlet is observed at 7.40 ppm. This variation in chemical shift is due to increase in electron density near H of imine.

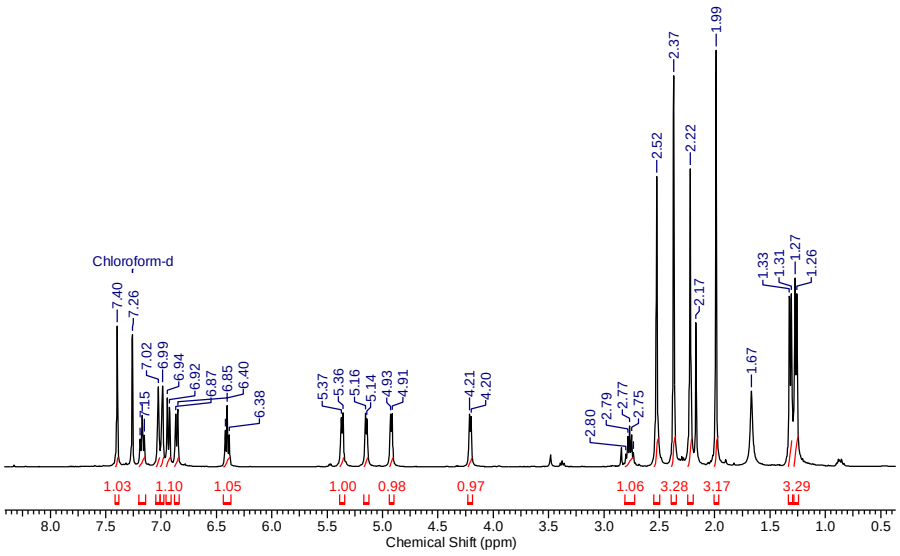

Figure 28: ^{1}H NMR spectrum of Complex C4.

3.3. Catalysis:

3.3.1. Dehydrogenation of aqueous formaldehyde:

Dehydrogenation of aqueous formaldehyde (13.55 mmol, 1.016 mL) was done by using Ru-arene complexes as catalyst at 95 ˚C as shown in scheme 18.

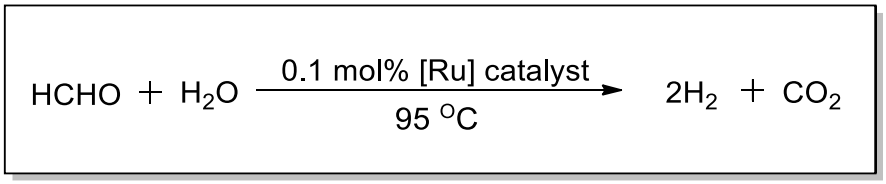

Scheme 18: Catalytic dehydrogenation of aq. formaldehyde.

The catalytic activity of C1, C2, C3 and C4 was checked at 95 ˚C for dehydrogenation of formaldehyde and volume of evolved gas was measured by using water displacement method. Calculated TON and TOF values are shown in table 1.

Catalyst	TON (20 min)	TOF (h^{-1}) (20 min)	TON (200 min)	TOF (h^{-1}) (In 200 min)
C1	286	859	593	178
C2	281	844	613	184
C3	341	1023	693	208
C4	316	948	593	178

Table 1: Catalytic table for dehydrogenation of aq. formaldehyde.

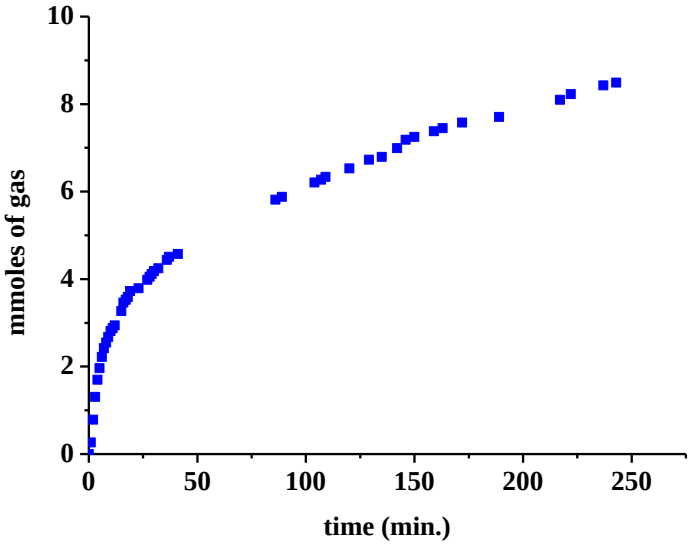

Figure 29 Plot of the mmoles of gas evolved by catalytic dehydrogenation of aq. HCHO *vs* time in presence of complex **C1**.

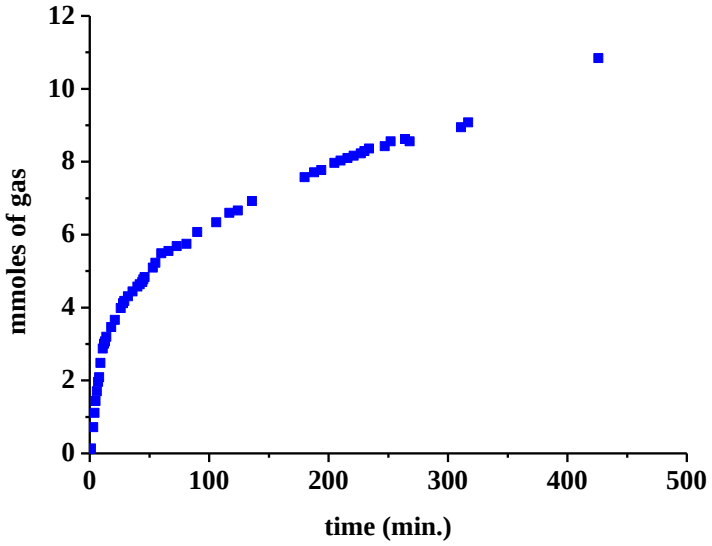

Figure 30: Plot of the mmoles of gas evolved by catalytic dehydrogenation of aq. HCHO *vs* time in presence of complex C2.

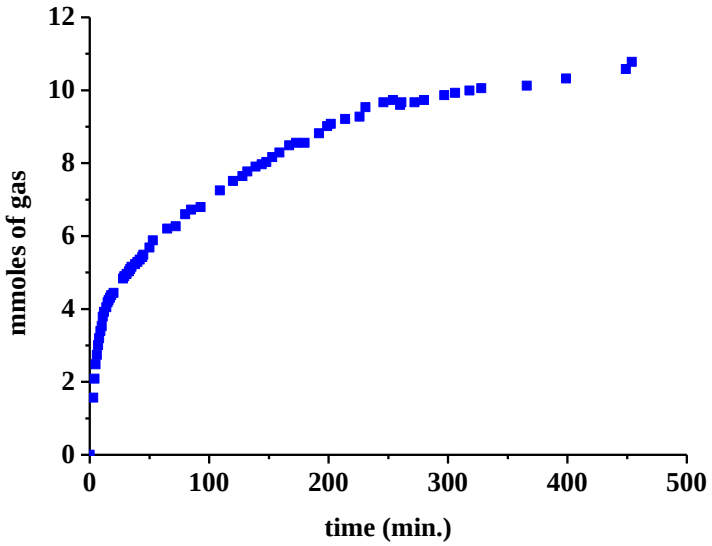

Figure 31 Plot of the mmoles of gas evolved by catalytic dehydrogenation of aq. HCHO *vs* time in presence of complex C3.

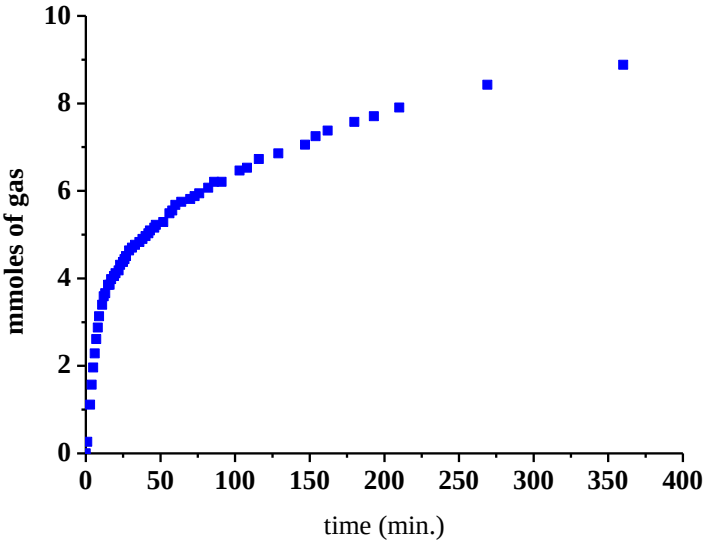

Figure 32: Plot of the mmoles of gas evolved by catalytic dehydrogenation of aq. HCHO *vs* time in presence of complex C4.

3.3.2. Dehydrogenation of formic acid:

Dehydrogenation of formic acid (10 mmol, 378 μL) was done by using C1 as a catalyst at 95 ˚C as shown in scheme 19.

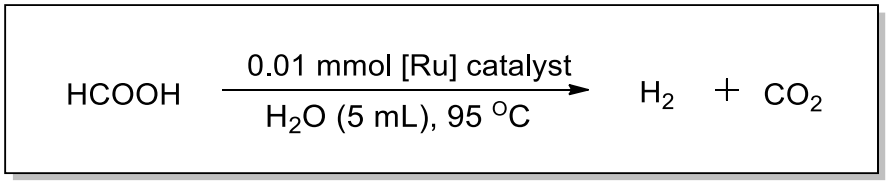

Scheme 19: Catalytic dehydrogenation of formic acid.

Catalytic dehydrogenation of formic acid is assumed to proceed through the plausible mechanism shown in scheme 20. For initial 10 minutes, calculated TON and TOF values are found to be TON = 98, TOF = 590 h^{-1}.

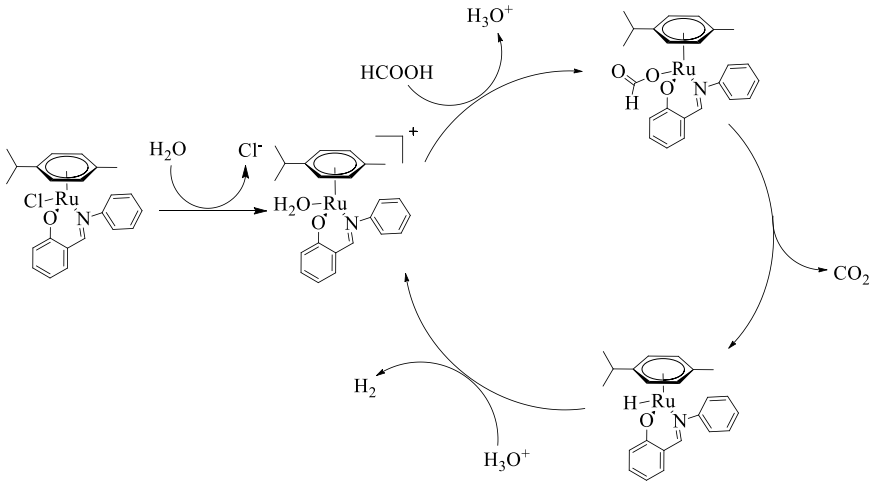

Scheme 20: Plausible mechanism for the catalytic dehydrogenation of formic acid.

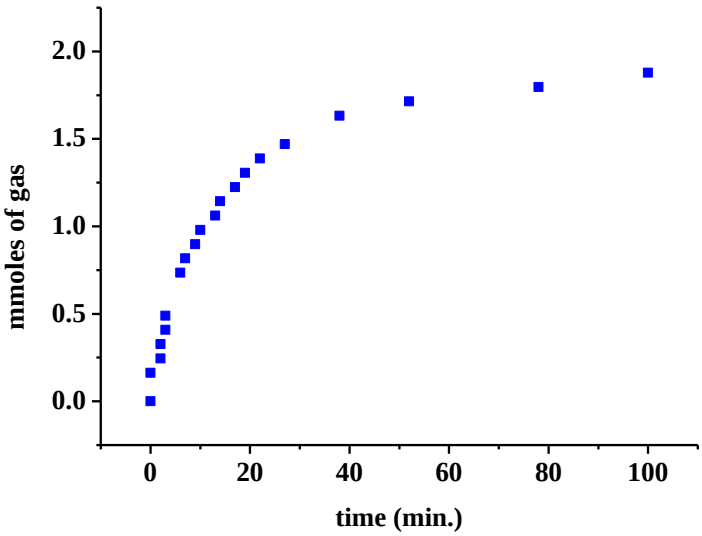

Figure 33 Plot of the mmoles of gas evolved by catalytic dehydrogenation of HCOOH *vs* time in presence of complex C1.

Chapter 4 Conclusion

4.1. Conclusion:

We have successfully synthesized the different arene ligands and their respective ruthenium complexes. All the synthesized products were characterized by NMR and mass spectrometry. Catalytic dehydrogenation of the formic acid and formaldehyde was done by using various synthesized complexes. TON and TOF values were calculated per ruthenium atom by using water displacement system.

4.2. Future scopes:

Further clarifications and modification are yet to be explored. The catalytic activity of these complexes can be improved by changing temperature conditions and by using a particular amount of base.

Complexes of the reduced ligands can also show better activity due to the presence of N-H moiety.

REFERENCES

[1] Johnson T. C., Morris D. J., Wills M. (2010), Hydrogen generation from formic acid and alcohols using homogeneous catalysts, Chem. Soc. Rev., 39, 81–88.

[2] Jacobson M. Z. (2009), Review of solutions to global warming, air pollution and energy security, Energy Environ. Sci., 2, 148–173.

[3] Bockris J. O'M. (1972), A Hydrogen Economy, Science, 176, 1323.

[4] Sartbaeva A., Kuznetsov V. L., Wells S. A., Edwards P. P. (2008) Hydrogen Nexus in a Sustainable Energy Future, Energy Environ. Sci., 1, 79−85.

[5] Zhang H., Shen P. K. (2012), Recent Development of Polymer Electrolyte Membranes for Fuel Cells, Chem. Rev., 112, 2780–2832.

[6] Pourbaba M., Zirakkar S. (2011), Utilization of renewable energy to produce electrical energy (Hydrogen Energy), Procedia Eng., 21, 1088–1095.

[7] Himeda Y. (2009), Highly efficient hydrogen evolution by decomposition of formic acid using an iridium catalyst with 4,4′-dihydroxy-2,2′-bipyridine, Green Chem., 11, 2018-2022.

[8] Olah G. A., Goeppert A., Prakash G. K. S. (2009), Beyond Oil and Gas: The Methanol Economy, 2nd ed.; Wiley-VCH: Weinheim.

[9] Dalebrook A. F., Gan W., Grasemann M., Moret S., Laurenczy G. (2013), Hydrogen storage: beyond conventional methods, Chem. Commun., 8735-8751.

[10] Yadav M., Xu Q. (2012), Liquid-phase chemical hydrogen storage materials, Energy Environ. Sci., 5, 9698-9725.

[11] Jiang H.L., Singh S. K., Yan J. M., Zhang X. B., Xu Q. (2010), Liquid-Phase Chemical Hydrogen Storage: Catalytic Hydrogen Generation under Ambient Conditions, ChemSusChem., 3, 541-549.

[12] Thomas K. M. (2009), Adsorption and desorption of hydrogen on metal-organic framework materials for storage applications: Comparison with other nanoporous materials, Dalton Trans., 1487–1505.

[13] Makowski P., Thomas A., Kuhn P., Goettmann F. (2009), Energy Environ. Sci., 2, 480–490.

[14] Demirci U. B., Miele P. (2009), Sodium borohydride versus ammonia borane, in hydrogen storage and direct fuel-cell applications, Energy Environ. Sci., 2, 627–637.

[15] Heim L. E., Schlörer N. E., Choi J. H., Prechtl M. H. G. (2014), Selective and Mild Hydrogen Production Using Water and Formaldehyde, Nat. Commun., 5, 3621.

[16] Heim L. E., Vallazza S., van der Waals D., Prechtl M. H. G. (2016), Water Decontamination with Hydrogen Production Using Microwave-formed Minute-made Ruthenium Catalysts, Green Chem., 18, 1469−1474.

[17] Suenobu T., Isaka Y., Shibata S., Fukuzumi S. (2015), Catalytic Hydrogen Production from Paraformaldehyde and Water Using an Organoiridium Complex, Chem. Commun., 51, 1670−1672.

[18] Fujita K. I., Kawahara R., Aikawa T., Yamaguchi R. (2015), Hydrogen Production from a Methanol−Water Solution Catalyzed by an Anionic Iridium Complex Bearing a Functional Bipyridonate Ligand under Weakly Basic Conditions, Angew. Chem., Int. Ed. 2015, 54, 9057−9060.

[19] Trincado M., Sinha V., Rodriguez-Lugo R. E., Pribanic B., de Bruin B., Grutzmacher H. (2017), Homogeneously catalysed Conversion of Aqueous Formaldehyde to H_2 and Carbonate, Nat. Commun., 8, 14990.

[20] Li R. H., Zhu X. H., Yan X. Q., Kobayashi H., Yoshida S., Chen W. X., Du L. L., Qian K. C., Wu B., Zou S., Lu L., Yi W., Zhou Y., Fan J. (2017), Oxygen-Controlled Hydrogen Evolution Reaction: Molecular Oxygen Promotes Hydrogen Production from Formaldehyde Solution Using Ag/MgO Nanocatalyst, ACS Catal., 7, 1478−1484.

[21] Grasemann M., Laurenczy G. (2012), Formic acid as a hydrogen source − recent developments and future trends, Energy Environ. Sci., 5, 8171−8181.

[22] Singh A. K., Singh S., Kumar A. (2016), Hydrogen energy future with formic acid: a renewable chemical hydrogen storage system Catal. Sci. Technol., 6, 12−40.

[23] Mellmann D., Sponholz P., Junge H., Beller M. (2016), Formic acid as a hydrogen storage material − development of homogeneous catalysts for selective hydrogen release, Chem. Soc. Rev., 45, 3954−3988.

[24] Eppinger J., Huang K.W. (2017), Formic Acid as a Hydrogen Energy Carrier, ACS Energy Lett., 2, 188−195.

[25] Sordakis K., Tang C., Vogt L. K., Junge H., Dyson P. J., Beller M., Laurenczy G. (2018), Homogeneous Catalysis for Sustainable

Hydrogen Storage in Formic Acid and Alcohols, Chem. Rev., 118, 372−433.

[26] Zhong H., Iguchi M., Chatterjee M., Himeda Y., Xu Q., Kawanami H. (2018), Formic Acid-Based Liquid Organic Hydrogen Carrier System with Heterogeneous Catalysts, Adv. Sustainable Syst., 2, 1700161.

[27] Sordakis K., Tang C., Vogt L. K., Junge H., Dyson P. J., Beller M., Laurenczy G. (2018), Homogeneous Catalysis for Sustainable Hydrogen Storage in Formic Acid and Alcohols, Chem. Rev., 118, 372−433.

[28] Wang L., Ertem M. Z., Kanega R., Murata K., Szalda D. J., Muckerman J. T., Fujita E., Himeda Y. (2018), Highly Efficient and Selective Methanol Production from Paraformaldehyde and Water at Room Temperature, ACS Catal., 8, 8600-8605.

[29] Guan C., Zhang D. D., Pan Y., Iguchi M., Ajitha M. J., Hu J., Li H., Yao C., Huang M. H., Min S., Zheng J., Himeda Y., Kawanami H., Huang K. W. (2017), Dehydrogenation of Formic Acid Catalyzed by a Ruthenium Complex with an N, N′-Diimine Ligand, Inorg. Chem., 56, 438−445.

[30] Guo J., Lin C., Jiang C., Zhang P. (2019), Review on noble metal-based catalysts for formaldehyde oxidation at room temperature. Applied Surface Science 475, 237–255.

[31] Iglesias M., Oro L. A. (2018), Eur. J. Inorg. Chem., 2125–2138.

[32] Matsunami A., Kayaki Y., Ikariya T. (2015), Chem. Eur. J., 21, 13513–13517;

[33] Oldenhof S., Lutz M., de Bruin B., van der Vlugt J. I., Reek J. N. H. (2015), Chem. Sci., 6, 1027–1034.

[34] Barnard J. H., Wang C., Berry N. G., Xiao J. L. (2013), Chem. Sci., 4, 1234–1244.

[35] Matsunami A., Kuwata S., Kayaki Y. (2017), ACS Catal., 7, 4479–4484.

[36] Wang W. H., Xu S., Manaka Y., Suna Y., Kambayashi H., Muckerman J. T., Fujita E., Himeda Y. (2014), ChemSusChem,7, 1976–1983.

[37] Li J., Zhang D., Liu C. (2016), ACS Catal., 6, 4746–4754.

[38] Coffey R. S. (1967), the decomposition of formic acid catalysed by soluble metal complexes, Chem. Commun., 923−924.

[39] Boddien A., Ga¨rtner F., Nielsen M., Losse S., Junge H., in Comprehensive Inorganic Chemistry II, ed. J. Reedijk and K. Poeppelmeier, Elsevier, Oxford, UK, 2013, pp. 587–603.

[40] Loges B., Boddien A., Ga¨rtner F., Junge H., Beller M. (2010), Top. Catal., 53, 902–914.

[41] Forster D., Beck G. R. (1971), J. Chem. Soc. D, 1072.

[42] Wiener H., Sasson Y., Blum J. (1986), J. Mol. Catal., 35, 277–284.

[43] Paonessa R. S., Trogler W. C. (1982), J. Am. Chem. Soc., 104, 3529–3530.

[44] Yoshida T., Ueda Y., Otsuka S. (1978), J. Am. Chem. Soc.,

100, 3941–3942.

[45] Patureau F. W., Kuil M., Sandee A. J., Reek J. N. H. (2008), Angew. Chem., Int. Ed., 47, 3180–3183.

[46] Rieckborn T. P., Huber E., Karakoc E., Prosenc M. H. (2010), Eur. J. Inorg. Chem., 4757–4761.

[47] Filonenko G. A., Putten R. V., Schulpen E. N., Hensen M. E. J., Pidko E. A. (2014), Highly Efficient Reversible Hydrogenation of Carbon Dioxide to Formates Using a Ruthenium PNP-Pincer Catalyst, ChemCatChem., 6, 1526.

[48] Hull J. F., Himeda Y., Wang W. H., Hashiguchi B., Periana R., Szalda D. J., Muckerman J. T., Fujita E. (2012), Reversible Hydrogen Storage Using CO_2 and a Proton-Switchable Iridium Catalyst in Aqueous Media Under Mild Temperatures and Pressures, Nat. chem., 4, 383.

[49] Manaka Y., Wang W. H., Suna Y., Kambayashi H., Muckerman J. T., Fujita E., Himeda Y. (2014), Catal. Sci.Technol., 4, 34.

[50] Wang W. H., Ertem M. Z., Xu S., Onishi N., Manaka Y., Suna Y., Kambayashi H., Muckerman J. T., Fujita E., Himeda Y. (2015), Highly Robust Hydrogen Generation by Bioinspired Ir Complexes for Dehydrogenation of Formic Acid in Water: Experimental and Theoretical Mechanistic Investigations at Different pH, ACS Catal., 5, 5496-5504.

[51] Papp G., Olveti G., Horvath H., Katho A., Joo F. (2016), Highly efficient dehydrogenation of formic acid in aqueous solution catalysed by an easily available water-soluble iridium(III) dihydride, Dalton trans., 45, 14516-14519.

[52] Patra S., Awasthi M. K., Rai R. K., Deka H., Mobin S. M., Singh S. K. (2019), Dehydrogenation of Formic Acid Catalyzed by Water-Soluble Ruthenium Complexes: X-ray Crystal Structure of a Diruthenium Complex, Eur. J. Inorg. Chem., 2019, 1046-1053.